

ExRET-Opt: An automated exergy/exergoeconomic simulation framework for building energy retrofit analysis and design optimisation

Iván García Kerdan^{a, c*}, Rokia Raslan^b, Paul Ruyssevelt^a, David Morillón Gálvez^c

^a Energy Institute, University College London, 14 Upper Woburn PI, London, WC1H 0NN, U.K.

^b Environmental Design and Engineering, University College London, 14 Upper Woburn PI, London, WC1H 0NN, U.K.

^c Departamento de Mecánica y Energía, Instituto de Ingeniería, Universidad Nacional Autónoma de México, México, México

Abstract

Energy simulation tools have a major role in the assessment of building energy retrofit (BER) measures. Exergoeconomic analysis and optimisation is a common practice in sectors such as the power generation and chemical processes, aiding engineers to obtain more energy-efficient and cost-effective energy systems designs. ExRET-Opt, a retrofit-oriented modular-based dynamic simulation framework has been developed by embedding a comprehensive exergy/exergoeconomic calculation method into a typical open-source building energy simulation tool (EnergyPlus). The aim of this paper is to show the decomposition of ExRET-Opt by presenting modules, submodules and subroutines used for the framework's development as well as verify the outputs with existing research data. In addition, the possibility to perform multi-objective optimisation analysis based on genetic-algorithms combined with multi-criteria decision making methods was included within the simulation framework. This addition could potentiate BER design teams to perform quick exergy/exergoeconomic optimisation, in order to find opportunities for thermodynamic improvements along the building's active and passive energy systems. The enhanced simulation framework is tested using a primary school building as a case study. Results demonstrate that the proposed simulation framework provide users with thermodynamic efficient and cost-effective designs, even under tight thermodynamic and economic constraints, suggesting its use in everyday BER practice.

Keywords:

building energy retrofit; exergy; exergoeconomics; building simulation software; optimisation.

*Corresponding author at: Energy Institute, University College London, United Kingdom. Tel: +44 (0) 7867798730

E-mail address: i.kerdan.12@ucl.ac.uk (I. Garcia Kerdan)

40 1. Introduction

41

42 Improving building energy efficiency through building energy retrofit (BER) is one of the most
43 effective ways to reduce energy use and associated pollutant emissions. From an economic
44 and environmental perspective, energy conservation and efficiency measures could hold
45 greater potential than deployment of renewable energy technologies [1]. Computational
46 modelling and simulation plays an important role in understanding complex interactions.
47 Building performance modelling and simulation is a fast flourishing field, focusing on reliable
48 reproduction of the physical phenomena of the built environment [2]. Several retrofit-oriented
49 simulation tools have been developed in the last two decades, commonly using as the main
50 energy calculation engine open source tools such as DOE 2.2® [3] and EnergyPlus® [4].
51 Among the most recent developments are ROBESim [5], CBES [6] and SLABE [7]. Rysanek
52 and Choudhary [8] developed an exhaustive retrofit simulation tool by coupling the transient
53 simulation tool TRNSYS® [9] with MatLab® [10], having the capability to simulate large set of
54 strategies under economic uncertainty.

55 Additionally, building energy design optimisation, an inherently complex, multi-disciplinary
56 technique, which involves many disciplines such as mathematics, engineering, environmental
57 science, economics, and computer science [11], is being extensively used in building design
58 practice. Attia et al. [12] found that 93% of multi-objective optimisation (MOO) research is
59 dedicated to early design; however, some studies have also demonstrated the strength of
60 MOO for BER projects [13-15]. Improvement of the envelope, HVAC equipment, renewable
61 generation, controls, etc., while optimising objectives, such as energy savings, occupant
62 comfort, total investment, and life cycle cost have been investigated. Among the most notable
63 contributions in applying MOO to BER design was Diakaki et al. [16]. The authors investigated
64 the feasibility of applying MOO techniques to obtain energy-efficient and cost-effective
65 solutions, with the objective of including the maximum possible number of measures and
66 variations in order to facilitate the project decision making. To date, the most popular available
67 MOO simulation tools are GenOpt, jEPlus, Tpgui, Opt-E-Plus, and BEOpt. Taking the
68 advantages from these tools, retrofit-oriented optimisation studies have become more common
69 in the last decade, considering different decision variables (retrofit measures), objective
70 functions, and constraints, while also investigating a wide range of mathematical algorithms.

71

72 2. Exergy and exergoeconomics

73 2.1 Exergy and buildings

74 Although widely accepted at scientific and practical levels in building energy design, typical
75 energy analysis (First Law of Thermodynamics) can have its limitations for an in depth
76 understanding of energy systems. Energy analysis cannot quantify real inefficiencies within
77 adiabatic processes and considers energy transfers and heat rejection to the environment as
78 a system thermodynamic inefficiency [17]. The main limitation of the First Law is that it does
79 not account for energy quality, where thermal, chemical, and electrical energy sources, should
80 not be valued the same, since they all have different characteristics and potentials to produce
81 work. Thereby, as a result of a notorious lack of thermodynamic awareness among buildings'
82 energy design, these presents poor thermodynamic performance with overall efficiencies
83 around 12% [18, 19]. Exergy, a concept based on the Second Law of Thermodynamics,
84 represents the ability of an energy carrier to perform work and is a core indicator of measuring
85 its quality. Therefore, the main difference between the First and the Second Law is the
86 capabilities of the latter to account for the different amount of exergy of every energy source
87 while also calculate irreversibilities or exergy destructions.

88 In some sectors, such as cryogenics [20], power generation [21], chemical and industrial
89 processes [22-23], and renewable energy conversion systems [24], exergy methods count with
90 a certain degree of maturity that makes the analysis useful in everyday practice. Some of these
91 methodologies have been supported with the development of simulation tools, especially in
92 the process engineering field. Montelongo-Luna et al. [22] developed an open-source exergy
93 calculator by integrating exergy analysis into Sim42®, an open-source chemical process
94 simulator. The tool has the potential to be applied into the early stages of process design and/or
95 retrofitting of industrial processes with the aim of locating sources of inefficiencies. Querol et
96 al. [23] developed a Visual Basic add-on to perform exergy and thermoeconomic analysis
97 with the support of Aspen Plus®, a commercial chemical process simulation software. The
98 aim was to aid the design process with an easy to use interface that allows the engineer to
99 study different alternatives of the same process. Later, Ghannadzadeh et al. [25] integrated an
100 exergy balance for chemical and thermal processes into ProSimPlus®, a process simulator for
101 energy efficiency analysis. The authors were capable of embedding the exergy subroutines
102 within the commercial tool without the necessity of external software, making the design
103 process easier for the engineer.

104 However, in buildings energy research, exergy analysis has been implemented at a slower
105 rate, and it is almost non-existent in the industry [26]. A limited number of building exergy-
106 based simulation tools have been developed with the intention to promote the concept of
107 exergy to a broader audience, especially directed towards educational purposes, common
108 practitioners, and decision makers. The first exergy-based building simulation tool can be

109 traced back to the work of the IEA EBC Annex 37 [27], where an analysis tool capable of
110 calculating exergy flows for the building energy supply chain was created. The tool was based
111 on a spreadsheet built up in different blocks of sub-systems representing each step of the
112 building energy supply chain. Based on this development, Sakulpipatsin and Schmidt [28]
113 included a GUI oriented towards engineers and architects. Later, for the IEA EBC Annex49
114 [29], the tool was improved along with the creation of other modules (S.E.P.E. and DVP). The
115 tool, called the '*LowEx pre-design tool*', is also a steady-state excel-based spreadsheet, but
116 enhanced with the use of macros and a more robust database for the analysis of more system
117 options. Schlueter and Thesseling [30] developed the GUI, with a focus to integrate exergy
118 analysis into a Building Information Modelling (BIM) software. Other modelling tools have been
119 developed for research purposes, where quasi-steady state or dynamic calculations have been
120 applied mainly with the support of TRANSYS simulation software [31, 32]. However, these
121 tools were developed to cover specific research questions and were not capable of rapidly
122 reproducing their capabilities for different designs.

123

124 *2.2 Exergoeconomics, optimisation and buildings*

125 Exergy analysis is a powerful tool to study interdependencies, and it is common that exergy
126 destructions within components are not only dependant on the component itself but on the
127 efficiency of the other system components [33]. Rocco et al. [34] concluded that the extended
128 exergy accounting method is a step forward to evaluate resource exploitation as it includes
129 socio-economic and environmental aspects expressed in exergy terms. By applying this
130 concept as optimisation parameter in a generic system, it provides a reduction of overall
131 resource consumption and larger monetary savings when compare to traditional economic
132 optimisation.

133 Exergy destructions or irreversibilities within the components have some cost implications,
134 therefore, would have an environmental and economic effect on the output streams. As exergy
135 is directly related to the physical state of the system, any negative impact would have an exergy
136 cost which leads to a more realistic appraisal than solely based on monetary costs. Therefore,
137 it can be said that exergoeconomics, and not simple economics (monetary cost), relates better
138 to the environmental impacts. Exergoeconomics can be an effective method for making
139 technical systems efficient by finding the most economical solution within the technically
140 possible limits [35]. In exergoeconomic analysis, depletion of high quality fuels combined with
141 low thermodynamic efficiencies is highly penalised, especially if the required energy demand
142 does not match the energy quality supply.

143 Among recent studies using exergoeconomics, Kohl et al. [36] investigated the performance
144 of three biomass-upgrading processes (wood pellets, torrefied wood pellets and pyrolysis
145 slurry) integrated into a municipal CHP plant. From an exergy perspective wood pellets was

146 the most efficient option; however, exergoeconomically, the pyrolysis slurry (PS) gave the
147 highest profits with a robust reaction against price fluctuations. With the projected future prices,
148 PS integration allows for the highest profit which a margin 2.1 times higher than for a stand-
149 alone plant without biomass upgrading. Mosaffa and Garousi Farshi [37] used
150 exergoeconomics to analyse a latent heat thermal storage unit and a refrigeration system. The
151 charging and discharging process of three different PCM were analysed from a second-law
152 perspective. Due to lowest investment cost rate of 0.026 M\$ and lowest amount of CO₂
153 emission, the PCM S27 with a length of 1.7m and a thickness of 10mm provided the lowest
154 total cost rate for the system (4094 \$/year). Wang et al. [38] applied exergoeconomics to
155 analyse two cogeneration cycles (sCO₂/tCO₂ and sCO₂/ORC) in which the waste heat from a
156 recompression supercritical CO₂ Brayton cycle is recovered for the generation of electricity.
157 Different ORC fluids were considered in the study (R123, R245fa, toluene, isobutane,
158 isopentane and cyclohexane). Exergy analysis revealed that the sCO₂/tCO₂ cycle had
159 comparable efficiency with the sCO₂/ORC cycle; however, when using exergoeconomics, the
160 total product unit cost of the sCO₂/ORC was slightly lower, finding that the isobutane had the
161 lowest total product unit cost (9.60 \$/GJ).

162

163 2.2.1 Exergoeconomic optimisation

164 An essential step when formulating exergoeconomic optimisation studies is the selection of
165 design variables that properly define the possible design options and affect system efficiency
166 and cost effectiveness [39]. Research have shown the importance of genetic algorithms (GA)
167 in energy design practice. GA combined with exergoeconomic optimisation has been
168 extensively used in thermodynamic-based research long time before. For example, Valdés et
169 al. [40] used thermoeconomics optimisation and GA to minimise production cost and maximise
170 annual cash flow of a combined cycle gas turbine. Mofid and Hamed [41] applied
171 exergoeconomic optimisation to a 140 MW gas turbine power plant taken as decision variables
172 the compressor pressure ratio and isentropic efficiency, turbine isentropic efficiency,
173 combustion product temperature, air mass flow rate, and fuel mass flow rate. Optimal designs
174 showed a potential to increase exergetic efficiency by 17.6% with a capital investment increase
175 of 8.8%. Ahmadi et al. [42] applied a NSGA-II using exergy efficiency and total cost rate of
176 product as objective functions to determine best parameters of a multi-generation system
177 capable of producing several commodities (heating, cooling, electricity, hot water and
178 hydrogen). Dong et al. [43] applied multi integer nonlinear programming (MINLP) and GA-
179 based exergoeconomic optimisation for a heat, mass and pressure exchange water distribution
180 network. A modified state space model was developed by the definition of superstructure.
181 However, the authors found that due to large number of variables, the GA was not efficient to
182 produce optimal results in a time-effective manner. Sadeghi et al. [44] optimised a trigeneration

183 system driven by a SOFC (solid oxide fuel cell) considering the system exergy efficiency and
184 total unit cost of products as objective functions recommending that the final design should be
185 selected from the Pareto front. Baghsheikhi et al. [45] applied real-time exergoeconomic
186 optimisation in form of a fuzzy inference system (FIS) with the intention to maximise the profit
187 of a power plant at different loads by controlling operational parameters. It was shown that the
188 FIS tool was faster and more accurate than the GA. Deslauriers et al [46] applied
189 exergoeconomic optimisation to retrofit a low temperature heat recovery system located in a
190 pulp and paper plant. The results showed significant steam operation cost reduction of up to
191 89% while reducing exergy destructions by 82%, giving the designer more options to be
192 considered than traditional heat exchanger design methods. Xia et al [47] applied
193 thermoeconomic optimisation of a combined cooling and power system based on a Brayton
194 Cycle (BC), an ORC and a refrigerator cycle for the utilisation of waste heat from the internal
195 combustion engine. The authors considered five key variables (compressor pressure ratio,
196 compressor inlet temperature, BC turbine inlet temperature, ORC turbine inlet pressure and
197 the ejector primary flow pressure) obtaining the lowest average cost per unit of exergy product
198 for the overall system. Recently, Ozcan and Dincer [48] applied exergoeconomic optimisation
199 of a four step magnesium-chlorine cycle (Mg-Cl) with HC1 capture. A thermoeconomic
200 optimization of the Mg-Cl cycle was conducted by using the multi-objective GA optimisation
201 within MATLAB. Optimal results showed an increase in exergy efficiency (56.3%), and a
202 decrease in total annual plant cost (\$409.3 million). Nevertheless, a big limitation of these
203 studies is the lack of an appropriate decision support tool for the selection of a final design,
204 leaving the decision to the judgement of the engineering.

205

206 *2.2.2 Exergoeconomics applied to building energy systems*

207 Despite the exergy-based building research developed in the last decade, the application of
208 exergoeconomics and exergoeconomic optimisation research oriented to buildings is limited.
209 The research from Robert Tozer [49, 50] can be regarded as the first buildings-oriented
210 thermoeconomic research showing its practical application to buildings' services. The author
211 presented an exergoeconomic analysis of different type of HVAC systems, locating those that
212 provide best thermodynamic performance. Later, Ozgener et al. [51] used exergoeconomics
213 to model and determine optimal design of a ground-source heat pump with vertical U-bend
214 heat exchangers. Ucar [52] used exergoeconomic analysis to find the optimal insulation
215 thickness in four different cities/climates in Turkey, using reference temperatures for the
216 analysis ranging from -21 °C to 3 °C. It was found that exergy destructions are minimised with
217 increasing insulation and ambient temperatures, but maximised with the increase of relative
218 indoor humidity. The variation of reference temperatures highly affects the thermoeconomic
219 outputs as these are strongly linked to exergy parameters, demonstrating the necessity to be

220 very careful if the analysis is performed using static or dynamic reference temperature [53].
221 Baldvinsson and Nakata [54] and Yücer and Hepbasli [55] applied the specific exergetic cost
222 (SPECOC) method for the analysis of different heating systems. Recently, Akbulut et al. [56]
223 applied exergoeconomic analysis to a GSHP connected to a wall cooling system calculating
224 exergy cost ranges for the compressor, condenser, undersoil heat exchanger, accumulator
225 tank and evaporator, finding an exergoeconomic factor value of the energy system of 77.68%.

226 Nevertheless, exergoeconomics can never replace long experience and knowledge of
227 technical economic theory. Therefore, tailored methods combining these approaches must be
228 developed. Exergy-based building simulation tools, despite having been created in the past
229 decade, lack exergoeconomic evaluation and an orientation to assess retrofit measures. As
230 shown in the literature, exergoeconomic-based multi-objective optimisations have proven to
231 be valuable for early design and retrofit projects in power plants and chemical processes with
232 common optimisation objectives such as cost, fuel cost, exergy destructions, exergy efficiency,
233 and CO₂ emissions; therefore, a potential exists for its implementation in building energy
234 design. As such, the aim of this paper is to expand the current knowledge in building energy
235 simulation and optimisation by presenting the details of ExRET-Opt, a building-oriented
236 exergoeconomic-based simulation framework for the assessment and optimisation of BER
237 designs, by showing the decomposition of the framework, and presenting modules,
238 submodules and subroutines used for the tool's development. Additionally, it is important to
239 show the application of exergoeconomic optimisation to a real case study, hoping that the
240 study would set the foundation for future similar studies.

241

242 **3. Calculation framework**

243 The basic exergy and exergoeconomic formulae together with an abstraction of the building
244 energy supply chain has been presented in previous publications [57, 58]. In this paper, the
245 methodological calculation has finally been integrated into a software, where the modules
246 details will be presented in the following sections.

247

248 *3.1 Exergy analysis*

249 To develop a holistic exergy building exergy analysis framework that considers most of the
250 energy systems located in a building, several exergy methodologies have been merged. For
251 the tool, calculations for thermal end uses and for renewable generations were taken from EBC
252 Annex49 [29] and Torio [59] with some modifications; while for electric-based energy flows,
253 the work from Rosen and Bulucea [60]. The developed holistic method provides with
254 comprehensive means to understand the interactions between the building envelope and the
255 building energy services (Fig. 1).

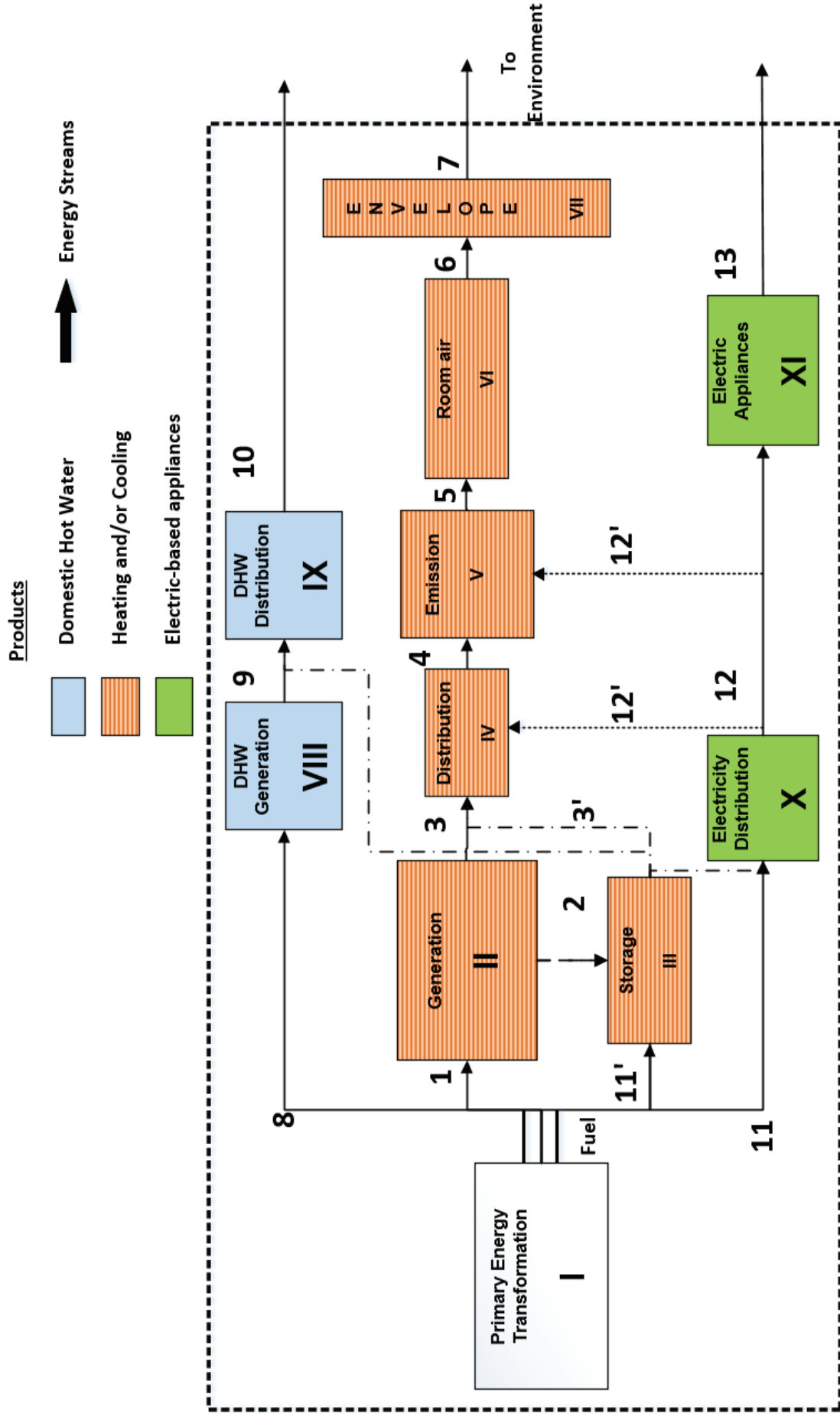


Fig. 1 Thermodynamic abstraction of a generic building energy chain in a building (HVAC, DHW, and electric appliances) [58]

258 3.2 Exergoeconomic analysis

259 From a wide range of thermoeconomic methods, the SPECO (specific exergy cost) method
260 [61, 62] was considered ideal for the proposed framework. It is considered the most adaptable
261 framework for BER due to its robustness and widely tested methodology in other energy
262 systems research. The method is based on the calculation of exergy efficiencies, exergy
263 destructions, exergy losses, and exergy ratios (destructions/inputs) at a component and
264 system level, giving the advantage of an ability to locate economically inefficient systems and
265 processes along the whole energy system. After identifying and calculating the exergy
266 streams, the method follows two main steps:

- 267 1. definition of fuel and product costs considering input cost, exergy destruction cost, and
268 increase in product costs, and,
- 269 2. identification of exergy cost equations.

270 However, for the SPECO method to be useful in BER design, a novel levelized
271 exergoeconomic index, the *exergoeconomic cost-benefit indicator* $Exec_{CB}$, has been
272 developed. This is calculated as follows:

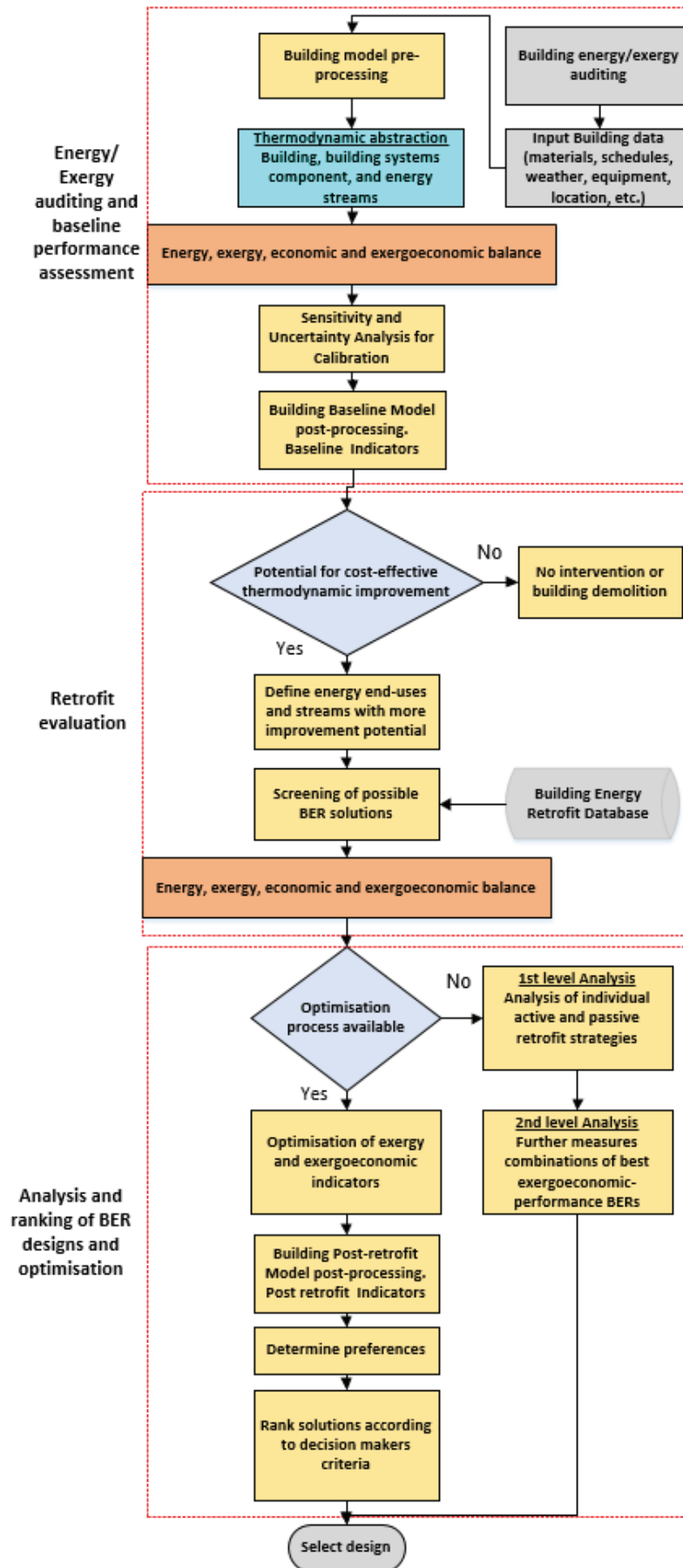
273
$$Exec_{CB} = \dot{C}_{D,sys} + \dot{Z}_{sys} - \dot{R} \quad (1)$$

274 where $\dot{C}_{D,sys}$ is the building's total exergy destruction cost, \dot{Z}_{sys} is the annual capital cost rate
275 for the retrofit measure, and \dot{R} is the annual revenue rate. All three parameters are levelized
276 considering the project's lifetime (50 years) and the present value of money. The outputs are
277 given in £/h. The indicator tries to solve the gap of integrating exergoeconomic evaluation in
278 typical economic analysis for BER design, by expressing exergy losses and its relative cost
279 into an indicator that is straightforward to understand. Specifically, for BER analysis, first, a
280 benchmark value has to be calculated for the pre-retrofitted building. This indicator will only be
281 composed of exergy destruction costs $\dot{C}_{D,sys,baseline}$ ($\dot{Z}_{sys}=0$ and $\dot{R}=0$). After the retrofit analysis
282 is performed, if the retrofitted building presents a $Exec_{CB}$ lower than the baseline $\dot{C}_{D,sys,baseline}$,
283 the design represents both a cost-effective solution and an improvement in exergy
284 performance.

285 *Exergy-efficient and cost-effective* $\rightarrow Exec_{CB} > \dot{C}_{D,sys,baseline}$

286 *Exergy-inefficient and cost-ineffective* $\rightarrow Exec_{CB} < \dot{C}_{D,sys,baseline}$

287 The proposed exergy/exergoeconomic framework aims to allow the practitioner to quantify the
288 First and Second Law parameters in order to locate more opportunities for improvement.
289 Several steps with different activities exist in common BER practice [63]. The proposed
290 framework, consists of three levels and is illustrated in Fig. 2.



291
292

Fig. 2 Exergy and exergoeconomic analysis methodology for BER

293 **4. ExRET-Opt simulation framework**

294 ExRET-Opt, a simulation framework consisting of several software subroutines, was
295 developed combining different modelling environments such as EnergyPlus, SimLab® [64],
296 Python® [65], and the Java-based jEPlus® [66] and jEPlus + EA® [67]. This software was
297 chosen for four main reasons:

- 298 a. Open source software that can be modified and adapted according to the research
299 necessities.
- 300 b. EnergyPlus was selected for First Law analysis as it is the most widely used building
301 performance simulation programme in academia and industry, allowing simulation of
302 HVAC systems and building envelope configurations.
- 303 c. Python programming language is ideal as a *scripting tool* for object-oriented system
304 languages, which also supports post-processing analysis by including data analysis
305 packages.
- 306 d. All chosen software has the ability to work with text based inputs/outputs which
307 facilitates the communication between the environments.

308 ExRET-Opt was designed to be modular and extensible. This framework gives the possibility
309 to study a wide range of BER measures and optimise designs under different objective
310 functions, such as energy and exergy use, exergy destructions and losses, exergy efficiency,
311 occupants' thermal comfort, operational CO₂ emissions, capital investment, life cycle cost,
312 exergoeconomic indicators, etc. The modelling engine is based on different existing modelling
313 environments and five modules:

314 **Module 1.** Input data and baseline building modelling

315 **Module 2.** Building model calibration

316 **Module 3.** Exergy and exergoeconomic analysis (and parametric study)

317 **Module 4.** Retrofit scenarios

318 **Module 5.** GA optimisation and MCDM

319 Additionally, ExRET-Opt has three operation modes:

320 Mode I. **Baseline evaluation:** A dynamic energy/exergy analysis and
321 economic/thermoeconomic evaluation is performed to obtain baseline values and
322 benchmarking data.

323 Mode II. **Parametric retrofit evaluation:** Using a comprehensive retrofit database, a
 324 parametric analysis can be performed for comparison and exploration of a wide range
 325 of active and passive retrofit measures

326 Mode III. **Optimisation:** Considering all possible combinations of retrofit measures, and
 327 based on constraints and objectives given by the user, ExRET-Opt can use a genetic
 328 algorithm-based optimisation procedure to search for close-to-optimal solutions in a
 329 time-effective manner

330 Depending of the operation mode, ExRET-Opt modules that are active are the following:

331 **Table 1 Active modules depending on ExRET-Opt operating mode**

| ExRET-Opt | Mode I | Mode II | Mode III |
|---|--------|---------|----------|
| Module 1: | | | |
| Input data and baseline building modelling | x | x | x |
| Module 2: | | | |
| Building model calibration | x | x | x |
| Module 3: | | | |
| Exergy and exergoeconomic analysis (and parametric study) | x | x | x |
| Module 4: | | | |
| Retrofit scenarios | | x | x |
| Module 5: | | | |
| MOGA optimisation and MCDM | | | x |

332 Following sections will focus on describing these modules in detail by explaining the simulation
 333 process involved and the coupling of different software environments and routines.

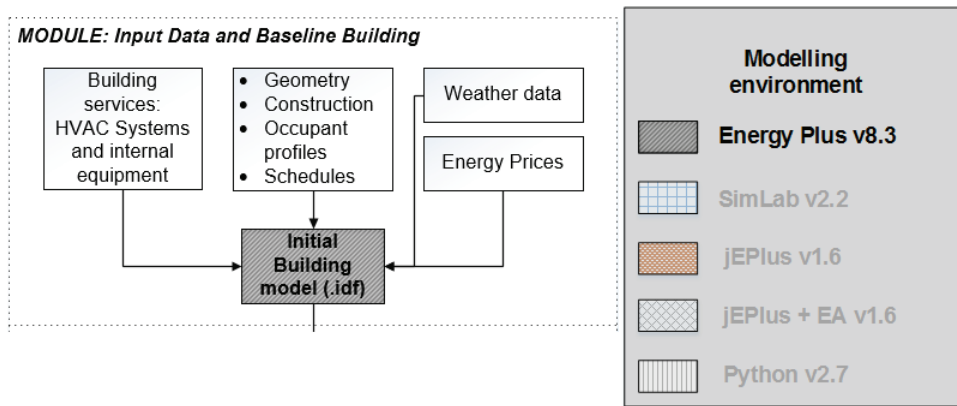
334

335 *4.1 Modules and process description*

336

337 *4.1.1 Module 1: Input data and baseline building modelling*

338 First, a pre-processing phase is involved were data collection, with regards to the building
 339 physical characteristics, occupancy profiles, energy systems, weather data, and energy prices,
 340 should be carried out, in order to construct a pre-calibrated baseline building model. A
 341 significant number of data sources is required for this specific task. Most common approaches
 342 are site visits and BMS data, which represent the best source of information. When data is
 343 missing or is hard to measure (i.e. occupancy levels, envelope thermal characteristics, internal
 344 heat gains, etc.), other sources of information, such as CIBSE [68] and ASHRAE [69] guides
 345 can be used to support the building modelling process [70]. Fig. 3 illustrates the modelling
 346 environments involved within this module.



347
348

Fig. 3 ExRET-Opt Module 1 simulation process

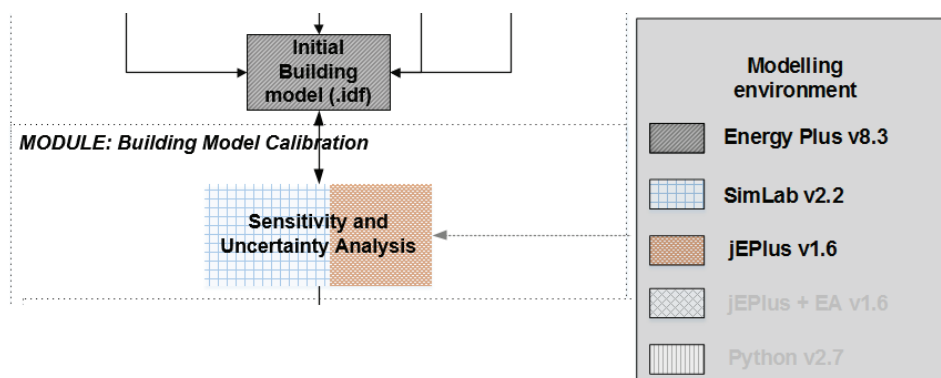
349 For the buildings' energy modelling, ExRET-Opt has its foundation on EnergyPlus 8.3. Its
350 biggest strength is the fact that it works with .txt files, which makes it possible to receive and
351 produce data in a generic text files form, making it easy to create third party add-ins.

352

353 *4.1.2 Module 2: Baseline building model calibration*

354 Considering the effects of uncertainties in building energy modelling, as a second step in the
355 modelling process, ExRET-Opt has included a 'calibration module'. The module was included
356 mainly for deterministic calibration purposes. For the calibration process, a three-software
357 process is required. Apart from EnergyPlus, both SimLab 2.2 and jEPlus 1.6.0 are necessary.
358 SimLab is a software designed for Monte Carlo (MC) based uncertainty and sensitivity
359 analysis, able to perform global sensitivity analysis, where multiple parameters can be varied
360 simultaneously and sensitivity is measured over the entire range of each input factor. On the
361 other hand, JEPlus is a Java-based open source tool, created to manage complex parametric
362 studies in EnergyPlus. Fig. 4 illustrates the module's process.

363



364
365

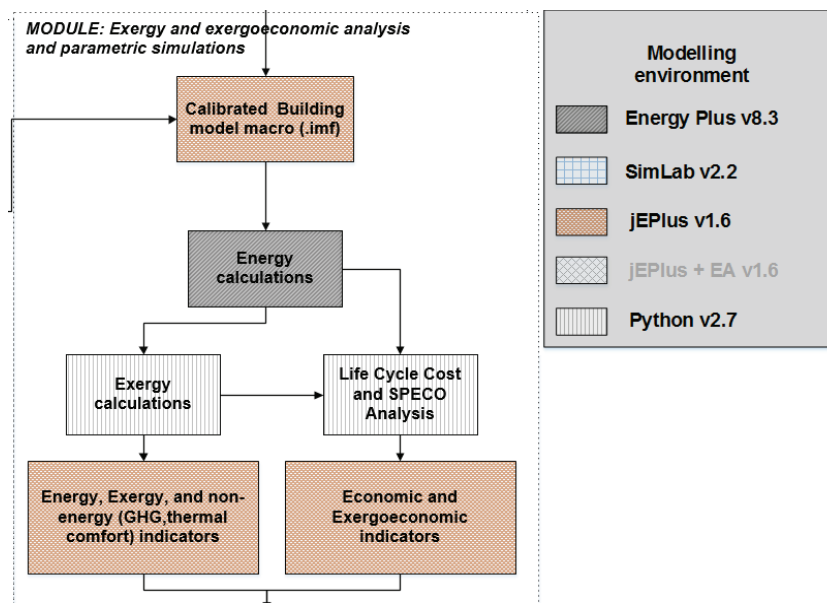
Fig. 4 ExRET-Opt Module 2 simulation process

366 The sampling method is based on Latin Hypercube Sampling (LHS) in order to keep the
367 number of required simulations at an acceptable level. SimLab creates a spreadsheet with the
368 new sample to be introduced to EnergyPlus. Then, with the aid of jEPlus, ExRET-Opt handles

369 the spreadsheet where the new EnergyPlus building models (.idf files) are created. Following,
 370 jEPlus passes the jobs to EnergyPlus for thermal simulation, where parallel simulation is
 371 available to make full use of all available computer processors. The final calibrated baseline
 372 energy model should meet the requirements of the ASHRAE Guideline 14-2002: *Measurement*
 373 *of Energy Demand and Savings* and is selected by having the lower Mean Bias Error (MBE)
 374 and Coefficient of Variation of the Root Mean Squared Error (CVRMSE).

375 **4.1.3 Module 3: Energy/Exergy and Exergoeconomic analysis**

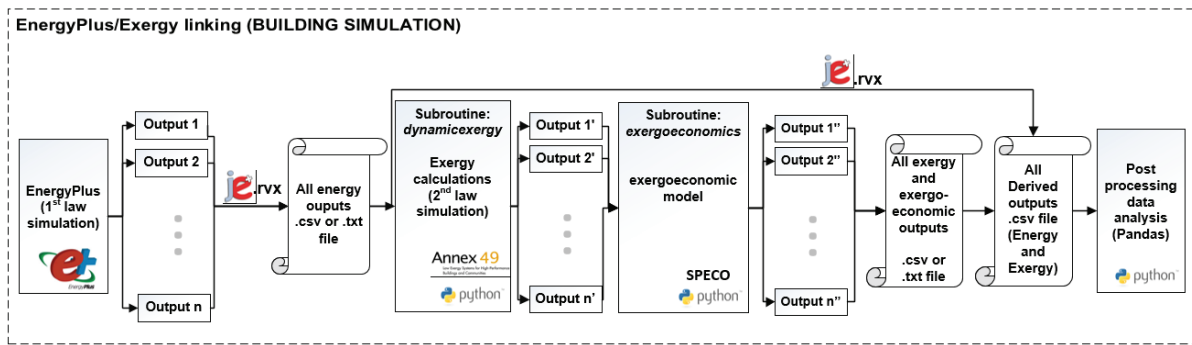
376 Undoubtedly, Module 3 can be considered as the most important main routine within ExRET-
 377 Opt. The entire modelling process of Module 3 is based on two subroutines: ‘subroutine:
 378 *dynamicexergy*’ and ‘subroutine: *exergoeconomics*’. The code of these subroutines is based
 379 on the mathematical formulae described in previous publications and that were further
 380 implemented in Python scripts. The strengths of Python programming language and the main
 381 reason of its integration in the tool is its modularity, code reuse, adaptability, reliability, and
 382 calculation speed [2]. Fig 5 illustrates the interaction among the different modelling
 383 environments involved in Module 3.



384
 385 **Fig. 5 ExRET-Opt Module 3 simulation process**

386 To further detail the module process, before ExRET-Opt calls the first subroutine, the reference
 387 environment has to be specified. As the exergy method only considers thermal exergy, the
 388 .epw weather file with hourly data on temperature and atmospheric pressure has to be used.
 389 Exergy analysis calculated by the ‘subroutine: *dynamicexergy*’, performs the analysis in the
 390 four different products of the building (heating, cooling, DHW, and electric appliances). This
 391 procedure is used to split the typical approach of a single stream analysis into multiple streams’
 392 analysis, able to calculate exergy indicators of each product in more detail. Following the end
 393 of the first subroutine, the ‘subroutine: *exergoeconomics*’ is called by ExRET-Opt and finally
 394 produces all the needed thermodynamic and thermoeconomic outputs.

395 For the integration of the subroutines into EnergyPlus, jEPlus is required. JEPlus latest
 396 versions provide users with the ability to use Python scripting for running own-made processing
 397 scripts, where communication between EnergyPlus and the Python-based exergy model is
 398 mainly supported through the use of .rvx files (extraction files data structure represented
 399 in JSON format). These files also allow the manipulation and handling of data back and forth
 400 among EnergyPlus, Python, and jEPlus. The detailed process of joining EnergyPlus and the
 401 developed subroutines is illustrated in Fig. 6.



402

403 **Fig. 6 Flow of Energy/Exergy co-simulation using EnergyPlus, Python scripting and jEPlus**

404 After both, 'subroutine: *dynamicexergy*' and 'subroutine: *exergoeconomics*' are called and
 405 calculations are performed, a new spreadsheet version is obtained with all the required
 406 outputs. The current version of the model is capable of providing 250+ outputs between
 407 energy, exergy, economic, exergoeconomic, environmental, and other non-energy indicators.

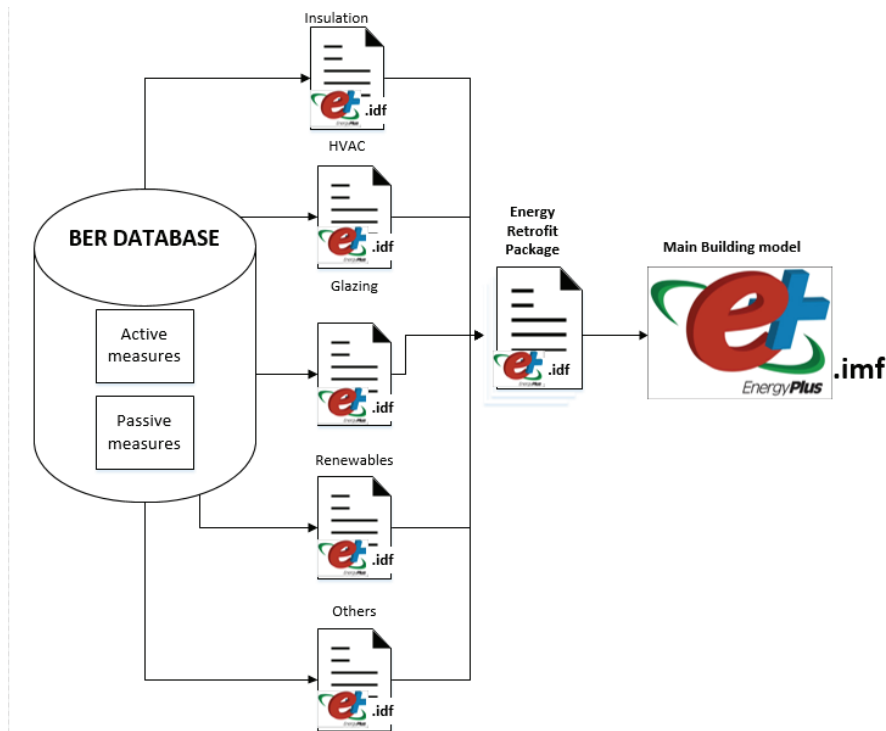
408

409 **4.1.4 Module 4: Retrofit scenarios and economic evaluation**

410 As building energy efficiency can usually be improved by both passive and active technologies,
 411 a comprehensive BER database including both technology types was compiled as part of the
 412 framework. This module encompasses a variety of retrofit measures (parameters) typically
 413 applied to non-domestic buildings in the UK and Europe [71, 72]. The module includes more
 414 than 100 individual energy saving measures. Consequently, attached prices are provided per
 415 unit (either kW or by m²) since the model automatically calculates the total capital price for
 416 either individual or combined measures. The list of technologies, variables, and prices¹ for all
 417 retrofit measures are detailed in Appendix A. To reduce economic uncertainties, several other
 418 considerations were included in the model such as future energy prices and government
 419 incentives (RHI and FiT). Depending on the retrofit technology, this could play a major role in
 420 the financial viability of some BER designs. To code each measure, these were implemented
 421 by developing individual stand-alone code recognisable ('.idf files') by EnergyPlus. Since the
 422 manual evaluation of retrofit measures is not feasible, ExRET-Opt uses parametric simulation

¹ If prices for some measures were not in local currency (GBP), conversion rates from 25th-October-2015 were considered.

423 to manipulate models, modify building model code, and simulate them. By using the EP-Macro
 424 function within EnergyPlus and coupling the process with jEPlus, it is possible to handle these
 425 'pieces of code' and introduce them into the main building model (Fig. 7).

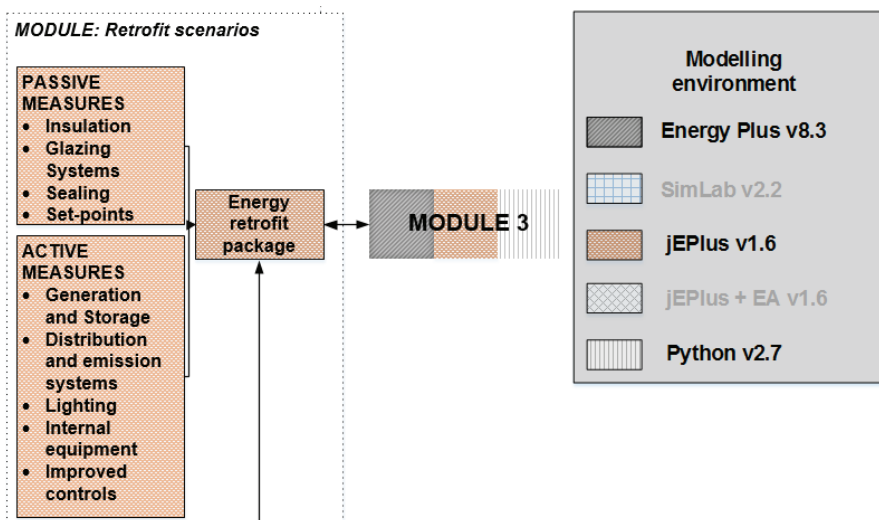


426
 427

Fig. 7 Building model construction using ExRET-Opt BER database

428 After the building model is finally constructed with its corresponding retrofit measures, including
 429 its techno-economic characteristics, a post-retrofit performance and prediction has to be
 430 performed. For this, ExRET-Opt Module 3 'subroutine: *dynamicexergy*' and 'subroutine:
 431 *exergoeconomics*', have to be called again. Fig. 8 illustrates the entire process of Module 4.

432



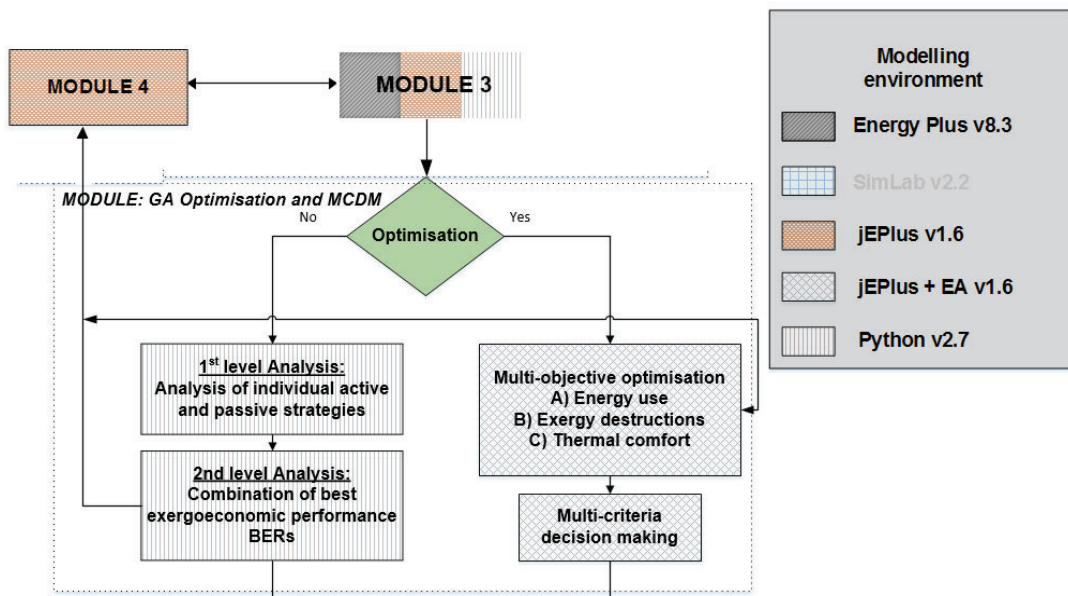
433
 434

Fig. 8 ExRET-Opt Module 4 simulation process

435 4.1.5 Module 5: Multi objective optimisation with NSGA-II and MCDM

436 Modules 3 and 4 have the capability to perform parametric or full-factorial simulations where
 437 an automation process of creating and simulating a large number of building models can be
 438 done. However, this process has its limitations, mainly depending on time constrains and
 439 computing power. For this reason, ExRET-Opt has the option of being used with an
 440 optimisation module, able to tackle multi-objective problems, reducing computing time, and
 441 achieving sub-optimal results in a time-effective manner.

442 To couple the framework with the optimisation module, a call function is required to
 443 automatically call the different generated building models, process the simulation, and return
 444 outputs for the subsequent energy/economic and exergy/exergoeconomic analysis. As seen
 445 in Fig. 9, this process is integrated within ExRET-Opt with the help of the Java platform
 446 JEPlus+EA. JEPlus+EA provides an interface with little configuration where the necessary
 447 controls (population size, crossover rate and mutation rate) are provided in the GUI or can be
 448 coded using Java commands. Meanwhile, the communication between platforms is done with
 449 the help of the .rvx file (JEPlus extraction file), where, in addition, objective functions and
 450 constraints have to be defined.



451
 452 **Fig. 9 ExRET-Opt Module 5 simulation process**

453 The advantages of using NSGA-II as the optimisation algorithm, is the ability to deal with large
 454 number of variables, ability for continuous or discrete variables' optimisation, simultaneous
 455 search from a large sample, and ability for parallel computing [73].

456

457 4.1.6 Module 5a: Solution ranking - MCDM submodule

458 The Pareto front(s) generated by Module 5 provides the decision maker with valuable
459 information about the trade-offs for the objectives involved. A method that can be used at this
460 stage to rank optimal solutions depending on the user's needs is Multi Criteria Decision Making
461 (MCDM). In ExRET-Opt, MCMD was included as a post-processing external module, where
462 Pareto solutions have to be exported to an Excel-based spreadsheet. For ExRET-Opt, similar
463 to Asadi et al. [14], compromise programming (CP) was selected as the MCDM method. CP
464 allows reducing the set of Pareto solutions to a more reasonable size, identifying an ideal or
465 utopian point which serves as a reference point for the decision maker. Thus, the decision
466 model has to be modified by including only one criterion. For this, a distance function has to
467 be analysed to find a set of solutions closest to the ideal point. This distance function is also
468 called Chebyshev distance and is defined as:

469
$$d_j = \frac{|Z_j^* - Z_j(x)|}{|Z_j^* - Z_{*j}|} \quad (2)$$

470

471 Where $Z_j(x)$ is the objective function, Z_j^* is the utopian point which represents the ideal minimum
472 solution, and Z_{*j} is the anti-ideal (nadir) point of the j th objective. The normalised degrees d_j
473 are expected to be between 0 and 1. If d_j is 0 it means that it has achieved its ideal solution.
474 On the other hand, if d_j achieves 1, the objective function is showing the anti-ideal or nadir
475 solution.

476 In practical terms, for compromise programming there is a need to know only the relative
477 preferences of the decision maker for each objective. This process can be done by the
478 weighted sum method. The method can transform multiple objectives into an aggregated
479 objective function. The corresponding weight factors (p_{ith}) reflect the relative importance of
480 each objective. This allows the decision maker to express the preferences by assigning a
481 number between 0 and 1 to each objective. However, the sum of weight coefficient has to
482 satisfy the following constraint:

483
$$\sum_{j=1}^n p_j = 1 \quad (3)$$

484

485 Therefore, the problem definition for compromise programming results in the following:

486
$$\alpha_j \geq \left(\frac{|Z_j^* - Z_j(x)|}{|Z_j^* - Z_{*j}|} \right) * (p_j) \quad (4)$$

487

488 where a minimisation of the Chebyshev distance α_j is sought.

489

490 **5. ExRET-Opt subroutines verification**

491

492 To ensure that ExRET-Opt is reliable, a validation or verification process is necessary. Due to
 493 lack of empirical exergy data, both an '*Inter-model Comparison*' using an existing tool and an
 494 '*Analytical Verification*' using various case studies found in the literature, are performed.

495

496 *5.1 Inter-model verification (steady-state analysis)*

497 The last version of the Annex 49 LowEx pre-design tool dates back in 2012. However,
 498 compared to ExRET-Opt, the LowEx tool lacks transient/dynamic calculation as it only relies
 499 on a steady-state energy balance analysis included in the spreadsheet. Additionally, it only
 500 considers heating and DHW as energy end-uses, lacking equations to calculate cooling and
 501 electric processes. Nevertheless, with the aim to test Module 3 within ExRET-Opt, steady-
 502 state calculations were performed. For the selection of the case study, the LowEx tool contains
 503 numerical examples of real pre-configured building cases. For this task '*The IEA SHC Task 25*
 504 *Office Building*' is selected. The steady-state analysis considers a reference temperature of 0
 505 °C and an internal temperature of 21 °C. The case studies input data can be seen in Table 2.

506

507 **Table 2 Input data for simulation (Annex 49 pre-design tool example building)**

| Baseline characteristics - A/C Office | Verification 1 |
|---------------------------------------|---|
| Case study | The IEA SHC Task25 Office Building |
| Number of floors | 1 |
| Floor space (m ²) | 929.27 |
| Orientation (°) | 0 |
| Air tightness (ach) | 0.6 |
| Exterior Walls | U _{value} =0.35 (W/m ² K) |
| Roof | U _{value} =0.17 (W/m ² K) |
| Ground floor | U _{value} =0.35 (W/m ² K) |
| Windows | U _{value} =1.10 (W/m ² K) |
| Glazing ratio | 32% |
| HVAC System | GSHP COP=3.5 |
| Emission system | Underfloor Heating: 40/30°C |
| Heating Set Point (°C) | 20.5 |
| Cooling Set Point (°C) | -- |
| Occupancy (people)* | 12.5 |
| Equipment (W/m ²)* | 1.36 |
| Lighting level (W/m ²)* | 2 |

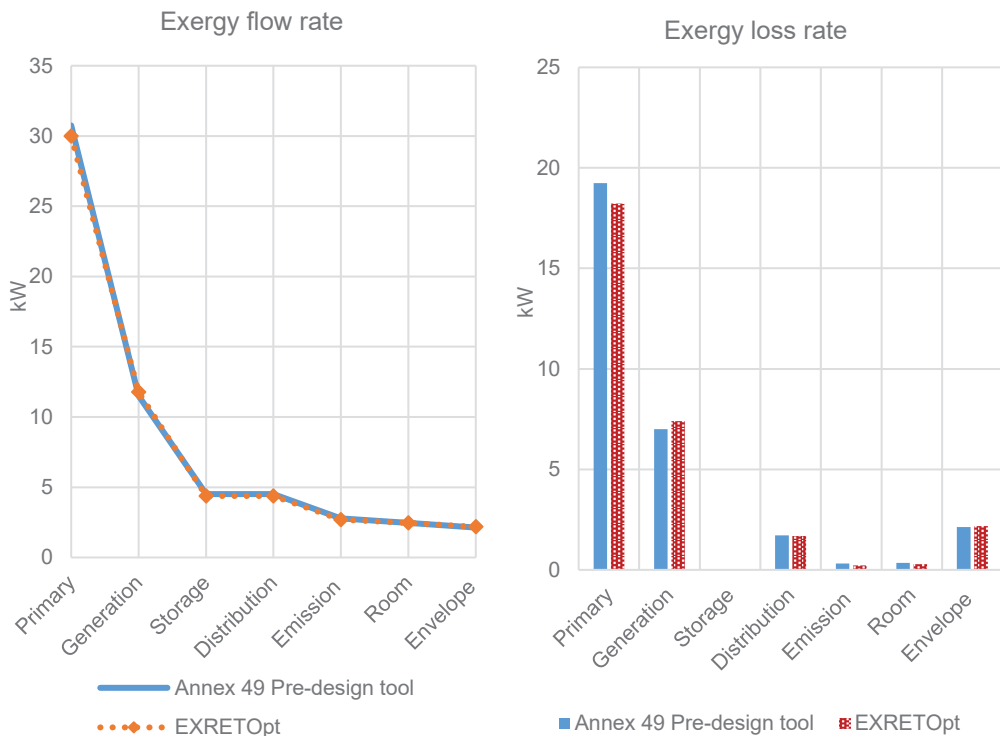
508 **5.1.1 Verification results**

509 The comparison between the tools' outputs, is given in Table 3. Deviations between
 510 outputs are no larger than 5% with similar results in assessing energy supply chain
 511 exergy efficiency.

512 **Table 3 Comparison of exergy rates results for inter-model verification**

| Subsystems | Annex 49 Pre-design tool | ExRET-Opt | Difference kW-(Deviation %) |
|--|---------------------------------|------------------|------------------------------------|
| <i>Envelope (kW)</i> | 2.13 | 2.18 | 0.05 (+2.3%) |
| <i>Room (kW)</i> | 2.47 | 2.47 | 0.00 (0.0%) |
| <i>Emission (kW)</i> | 2.79 | 2.69 | 0.10 (-3.6%) |
| <i>Distribution (kW)</i> | 4.51 | 4.37 | 0.14 (-3.1%) |
| <i>Storage (kW)</i> | 4.51 | 4.37 | 0.14 (-3.1%) |
| <i>Generation (kW)</i> | 11.51 | 11.77 | 0.26 (+2.3%) |
| <i>Primary (kW)</i> | 30.75 | 30.00 | 0.75 (-2.4%) |
| <i>Exergy efficiency ψ</i> | 6.95% | 7.26% | -- |

513 Fig. 10 shows the exergy flow rate and the exergy loss rate by subsystems. As can be noted,
 514 no larger differences exist, and the model under steady-state conditions performs well.



515 **Fig. 10 Comparison of exergy flow rates and exergy loss rates by subsystems**

517

518 By looking at the inter-model verification, it can be concluded that ExRET-Opt under steady-
 519 state calculation presents comprehensive results.

520 5.2 Analytical verification of subroutines

521 For the analytical verification, ExRET-Opt is compared against two numerical examples from
 522 the literature. The intention of this analysis is to verify the two 'Module 3' subroutines separately
 523 ('subroutine: *dynamicexergy*' and 'subroutine: *exergoeconomics*'). Although the research in
 524 dynamic building exergy and exergoeconomic analyses is limited, two highly cited articles can
 525 be relied on. Sakulpipatsin et al. [31] work can be used to verify the dynamic exergy analysis
 526 outputs, while Yücer and Hepbasli [55] work to verify exergoeconomic outputs.

527

528 5.2.1 Dynamic exergy analysis verification and results

529 Sakulpipatsin et al. [31] presented an exploratory work showing the application of dynamic
 530 exergy analysis in a single-zone model. These dynamic calculations were implemented in
 531 TRNSYS dynamic simulation tool. The case study building is a cubic-box with a net floor area
 532 of 300 m² spread along 3 stories. The heating system is based on district heating supplying
 533 hot water at 90 °C. The cooling system is based on a small-scale chiller with a COP of 1.5.
 534 Both systems supply the thermal energy to a low-temperature heating/high-temperature
 535 cooling panels. For the reference temperature, the De Bilt, Netherlands weather file is used as
 536 it was the reference weather file used in the original research. The full input data of the building
 537 and its HVAC system can be seen in Table 4.

538 **Table 4 Input data for analytical verification of subroutine: *dynamicexergy* within ExRET-Opt**

| Baseline characteristics A/C Office | Verification |
|---|---|
| <i>Case study</i> | Office building |
| <i>Location</i> | De Bilt, Netherlands |
| <i>Number of floors</i> | 3 |
| <i>Floor space (m²)</i> | 300 |
| <i>Orientation (°)</i> | 0 |
| <i>Air tightness (ach)</i> | 0.6 |
| <i>Natural ventilation rate (m³/h)/m³</i> | 4 |
| <i>Exterior Walls</i> | U-value=0.511 (W/m ² K) |
| <i>Roof</i> | U-value=0.316 (W/m ² K) |
| <i>Ground floor</i> | U-value=0.040 (W/m ² K) |
| <i>Windows</i> | U-value=1.300 (W/m ² K) |
| <i>Glazing ratio</i> | 42.5% (south façade only) |
| <i>HVAC System</i> | Heating: District Heating, T: 90 Cooling: Small Chiller COP: 1.5 (In both cases, distribution pipes have a temperature drop of 10 °C) |
| <i>Emission system</i> | Low temperature Heating: 35/28°C High Temperature Cooling: 10/23 °C |
| <i>Heating Set Point (°C)</i> | 20 |
| <i>Cooling Set Point (°C)</i> | 24 |
| <i>Occupancy (people)*</i> | 30 (75 W per person) |
| <i>Equipment (W/m²)*</i> | 23 |
| <i>Lighting level (W/m²)*</i> | 1.33 |

539 Table 5 compares two groups of data (heating and cooling) between the research data and
 540 ExRET-Opt outputs. The results show the exergy demand at each part of the supply chain,
 541 considering auxiliary energy for the HVAC system components. The corresponding differences
 542 in absolute value and in percentage are also shown. Results show that ExRET-Opt is capable
 543 of accurately predicting the heating exergy performance of the system. In the cooling case,
 544 larger deviations' percentage can be noted, mainly due to lower values, where small absolute
 545 value discrepancies can represent larger deviations. If compared to the heating case, the
 546 absolute values for cooling are much lower. However, since different weather files are used,
 547 the outputs seem reasonable. Nevertheless, efficiency values are rather similar.

548 **Table 5 Comparison of annual exergy use results for analytical verification of ExRET-Opt**

| | Sakulpipatsin et al. [31] | ExRET-Opt | Difference - (Deviation %) |
|--|---------------------------|-----------|----------------------------|
| Heating case | | | |
| Subsystems | | | |
| Building (kWh/m ² -y) | 5.66 | 4.51 | 1.15 (-20.31%) |
| Emission (kWh/m ² -y) | 16.17 | 13.93 | 2.24 (-16.6%) |
| Distribution (kWh/m ² -y) | 19.57 | 16.46 | 3.11 (-15.9%) |
| Primary Generation (kWh/m ² -y) | 33.03 | 33.78 | 0.75 (+1.14%) |
| <i>Exergy efficiency Ψ</i> | 17.13% | 13.35% | -- |
| Cooling case | | | |
| Subsystems | | | |
| Building (kWh/m ² -y) | 0.17 | 0.37 | 0.20 (+117.6%) |
| Emission (kWh/m ² -y) | 0.25 | 0.80 | 0.55 (+220.0%) |
| Distribution (kWh/m ² -y) | 0.33 | 0.88 | 0.55 (+166.6%) |
| Primary Generation (kWh/m ² -y) | 2.63 | 4.39 | 1.76 (+66.9%) |
| <i>Exergy efficiency Ψ</i> | 6.46% | 5.95% | -- |

549 Considering that the analysis is done at an hourly rate, the 'subroutine: *dynamicexergy*' seems
 550 to provide reliable results. However, the cooling calculations need further testing.

551

552 5.2.2 Exergoeconomics verification and results

553 In existing relevant literature, no comprehensive example of a dynamic exergy analysis
 554 combined with an exergoeconomic analysis applied to a building exists. However, Yücer and
 555 Hepbasli [55] performed a steady-state exergy and exergoeconomic analysis of a building's
 556 heating system, based on the SPECO method. The limitation of this research is that the exergy
 557 outputs are presented for just one temperature, neglecting the dynamism of an actual
 558 reference environment. For the case study, a house accommodation of 650 m² is considered.
 559 The reference environment is taken as 0 °C, with an internal temperature of 21 °C. The HVAC

560 system is composed of a steam boiler, using fuel oil that provides thermal energy to panel
 561 radiators to finally heat the room. Solar and internal heat gains have been neglected. The
 562 characteristics of the case study can be seen in Table 6.

563 **Table 6 Input data for analytical verification of subroutine: exergoeconomics within ExRET-Opt**

| Baseline characteristics A/C Office | Verification |
|---|--|
| <i>Case study</i> | House accommodation building |
| <i>Location</i> | Izmir, Turkey |
| <i>Number of floors</i> | 3 |
| <i>Floor space (m²)</i> | 650 |
| <i>Orientation (°)</i> | 0 |
| <i>Air tightness (ach)</i> | 1.0 |
| <i>Natural ventilation rate (m³/h)/m³</i> | -- |
| <i>Exterior Walls</i> | U _{value} =0.96 (W/m ² K) |
| <i>Roof</i> | U _{value} =0.43 (W/m ² K) |
| <i>Ground floor</i> | U _{value} =0.80 (W/m ² K) |
| <i>Windows</i> | -- |
| <i>Glazing ratio</i> | -- |
| <i>HVAC System</i> | Heating: Oil Boiler, T: 110 °C (Distribution pipes have a temperature drop < 10 °C) |
| <i>Emission system</i> | Radiator panels Heating: 35/28°C |
| <i>Heating Set Point (°C)</i> | 21 |
| <i>Cooling Set Point (°C)</i> | -- |
| <i>Occupancy (people)*</i> | -- |
| <i>Equipment (W/m²)*</i> | -- |
| <i>Lighting level (W/m²)*</i> | -- |

564 However, another limitation exists for the exergoeconomic analysis, as the authors have
 565 reduced the subsystems' analysis from seven to just three: generation, distribution, and
 566 emission subsystems. Since the capital cost of the subsystem is essential for this analysis, this
 567 is provided in Table 7.

568

569

Table 7 Components capital cost of the building HVAC system

| Subsystems | Capital cost (\$)² |
|---------------------------|--------------------------------------|
| <i>Distribution pipes</i> | 3,278 |
| <i>Radiator panels</i> | 5,728 |
| <i>Steam boiler</i> | 13,810 |
| <i>Envelope</i> | 3,959 |

570 The exergy price of the fuel is fundamental for exergoeconomic analysis as is it the product
 571 price entering the analysed stream. Only the heating mode is analysed, where fuel oil is

² Monetary values (USD) given as per original source

572 utilised. As the energy quality for oil is set at 1.0, both the energy price and exergy price are
 573 considered similar (0.096 \$/kWh).

574 Table summarises the results for this verification. First, a comparison of the steady-state exergy
 575 analysis is done to ensure that exergy values are within acceptable range. Some deviations
 576 are found, with the greatest at the room air subsystem (31.9%). However, as the deviations
 577 for the other subsystems are lower and the overall exergy efficiency of the whole system is
 578 similar, the obtained results seem acceptable.

579 **Table 8 Comparison of exergy rates results for subroutine: exergoeconomics verification**

| Subsystems | Yücer and Hepbasli [55] | ExRET-Opt Exergy analysis | Difference (Deviation %) |
|--------------------------|----------------------------|------------------------------|-----------------------------|
| Envelope (kW) | 3.78 | 3.11 | 0.67 (-17.7%) |
| Room (kW) | 11.93 | 8.13 | 3.80 (-31.9%) |
| Emission (kW) | 12.61 | 13.20 | 0.61 (-4.6%) |
| Distribution (kW) | 17.15 | 18.09 | 0.94 (+5.5%) |
| Generation (kW) | 82.38 | 94.98 | -12.60 (+15.3%) |
| Primary (kW) | 107.09 | 101.44 | -5.65 (-5.3%) |
| Exergy efficiency Ψ | 3.53% | 3.06% | -- |

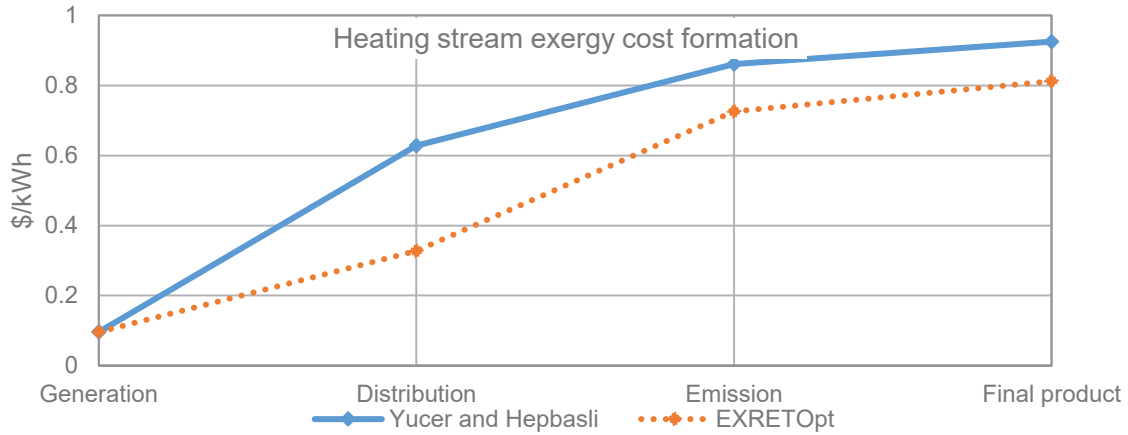
580

581 Table shows the verification of the exergoeconomic outputs for the reduced system analysis.
 582 Cost of fuels and products at each stage of the energy supply chain presented a similar
 583 increase trend. However due the simplicity of the steady-state approach by Yücer and Hepbasli
 584 [55], a great part of exergy destruction cost is not accounted correctly. On the other hand,
 585 ExRET-Opt calculates the exergy cost formation throughout the whole thermal energy supply
 586 chain.

587 **Table 9 Exergoeconomic comparison between research and ExRET-Opt**

| Subsystems | Yücer and Hepbasli [55] Exergoeconomic analysis | | | ExRET-Opt Exergoeconomic analysis | | | Difference (Deviation %) | | |
|--------------|--|-----------|----------------------|---|-----------|----------------------|-----------------------------|----------------|----------------------|
| | C, product \$/kWh | Z \$/h | C, fuel \$/kWh | C, product \$/kWh | Z \$/h | C, fuel \$/kWh | C, product \$/kWh | Z \$/h | C, fuel \$/kWh |
| | Generation | 0.096 | 0.46 | 0.628 | 0.096 | 0.44 | 0.327 | 0.00 (0.0%) | 0.02 (-4.3%) |
| Distribution | 0.628 | 0.07 | 0.861 | 0.327 | 0.07 | 0.726 | 0.301 (-48.1%) | 0.00 (0.0%) | 0.135 (-15.7%) |
| Emission | 0.861 | 0.17 | 0.925 | 0.726 | 0.18 | 0.812 | 0.135 (-15.7%) | .01 (+5.9%) | .0113 (-12.2%) |

588 Fig. 11 illustrates the stream cost increase comparison. The exergy cost formation increase is
 589 due to the system inefficiencies in the energy supply system with high volumes of exergy
 590 destructions. At each stage, an amount of economic value is added to the energy stream when
 591 it passes the energy supply chain.



592 **Fig. 11 Exergoeconomic cost increase of the stream**

594 Although the graph shows a similar behaviour, the deviations can be related to several factors.
 595 One is that ExRET-Opt performs the calculation for a supply chain composed of 7 subsystems,
 596 so exergy formation is more detailed and considers inefficiencies of different type of
 597 equipment. Another factor, is that the author does not mention the number of hours that the
 598 equipment is working, which affects the capital cost rate (\dot{Z}) and thus affects the exergy cost
 599 formation of the stream. However, final cost deviation was only found at 12.2%.

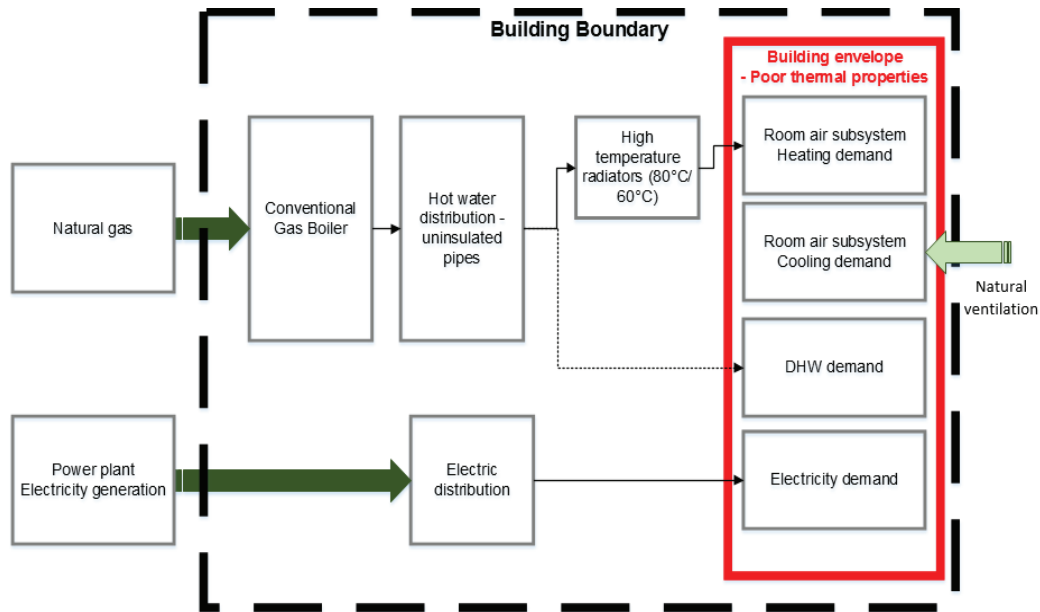
600

601 **6. ExRET-Opt application**

602

603 *6.1 Case study and baseline values*

604 To demonstrate ExRET-Opt capabilities, this has been applied to recently retrofitted primary
 605 school building (1900 m²) located in London, UK. The simulation model consists of a fourteen-
 606 thermal zone building. The largest proportion of the floor area is occupied by classrooms, staff
 607 offices, laboratories, and the main hall. Other minor zones include corridors, bathrooms, and
 608 other common rooms. Heating is provided by means of conventional gas boiler and high
 609 temperature radiators (80°C/60°C) with no heat recovery system. As no artificial cooling
 610 system is regarded, natural ventilation is considered during summer months. A schematic
 611 layout of the building energy system is illustrated in Fig. 12. Buildings thermal properties as
 612 well as energy benchmark indices are presented in Table 10. Properties such as occupancy
 613 schedules and inputs as well as environmental values are taken from the UK NCM [74] and
 614 Bull et al. [75].



615

616

Fig. 12 Schematic layout of the energy system for the Primary School base case

617

Table 10 Primary school baseline building model characteristics

| Baseline characteristics | Primary School |
|--|---|
| Year of construction | 1960s |
| Number of floors | 2 |
| Floor space (m ²) | 1,990 |
| Orientation (°) ⁺ | 227 |
| Air tightness (ach) ⁺ | 1.0 |
| Exterior Walls ⁺ | Cavity Wall-Brick walls 100 mm brick with 25mm air gap U _{value} =1.66 (W/m ² K) |
| Roof ⁺ | 200mm concrete block U _{value} =3.12 (W/m ² K) |
| Ground floor ⁺ | 150mm concrete slab U _{value} =1.31 (W/m ² K) |
| Windows ⁺ | Single-pane clear (5mm thick) U _{value} =5.84 (W/m ² K) |
| Glazing ratio | 28% |
| HVAC System ⁺ | Gas-fired boiler 515 kW η = 82% No cooling system |
| Emission system | Heating: HT Radiators 90/70°C Cooling: Natural ventilation |
| Heating Set Point (°C) ⁺ | 19.3 |
| Cooling Set Point (°C) ⁺ | -- |
| Occupancy (people/m ²) ^{**} | 2.1 |
| Equipment (W/m ²) ^{**} | 2.0 |
| Lighting level (W/m ²) ^{**} | 12.2 |
| EUI electricity (kWh/m ² -y) | 45.6 |
| EUI gas (kWh/m ² -y) | 142.3 |
| Annual energy bill (£/y) | 19,449 |
| Thermal discomfort (hours) | 1,443 |
| CO ₂ emissions (Tonnes) | 214.8 |

618 By end-use, heating represents 58.1% of the total energy demand, meaning that the 515 kW
 619 gas fired boiler consumes 781.7 GJ/year of natural gas. This is followed by 238.2 GJ/year for
 620 DHW (17.7%) and 59.0 GJ/year of electricity for interior lighting (13.7%). Fans, mainly used
 621 for mechanical cooling and extraction also have an intensive use, demanding 66.1 GJ/year,
 622 representing 4.9% of the total energy demand.

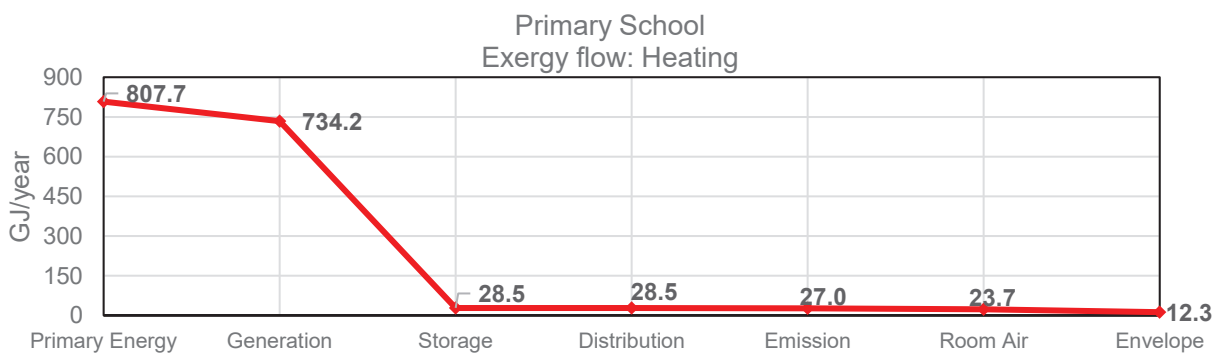
623 The outputs from the economic analysis deliver an annual energy bill of £19,449.3 for the
 624 building, where £10,949.6 is needed to cover electricity demand and £8,499.6 for natural gas.
 625 In addition, the LCC (over 50 years) obtained is found at £500,425 (£251.5/m²).

626

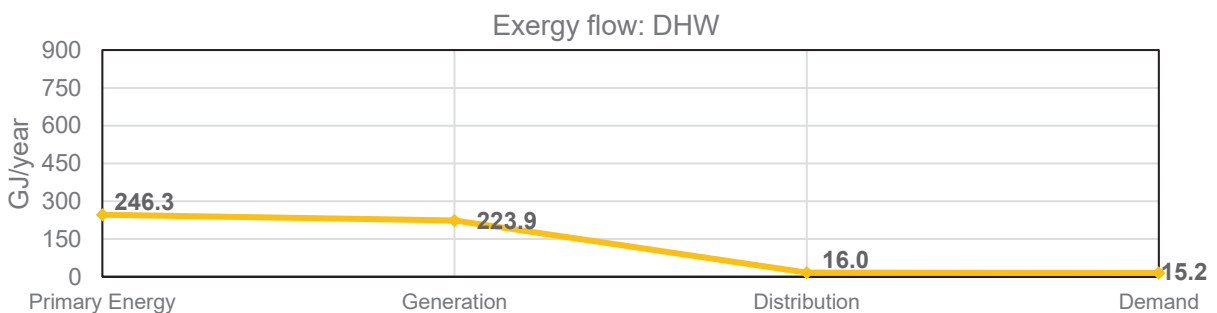
627 *6.1.1 Primary School baseline exergy flows and exergoeconomic values*

628 The building requires a total primary exergy input of 1,915.9 GJ/year (264.4 kWh/m²-year). By
 629 product type, electric-based equipment requires the largest share of 861.9 GJ (45%), followed
 630 by heating with 807.7 GJ (42.2%) and DHW with 246.3 GJ (12.8%). Fig. 13 shows the annual
 631 exergy flows for the three products analysed. Exergy flow diagrams give a first insight in the
 632 exergy behaviour inside the different building energy systems.

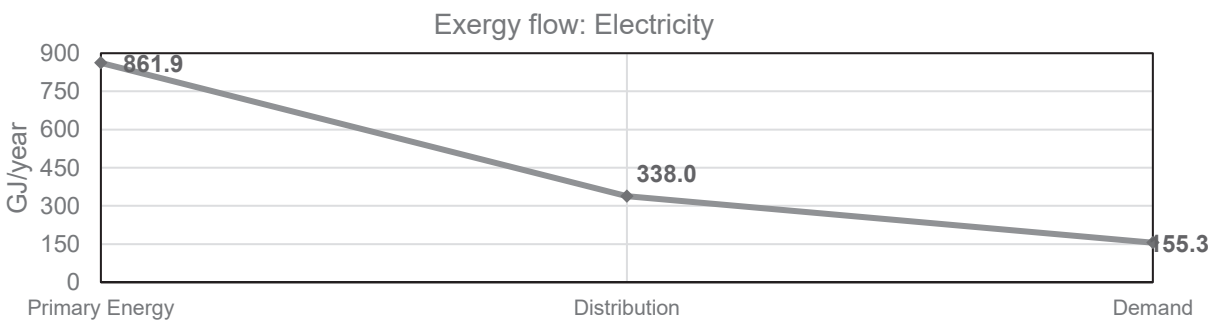
633



634



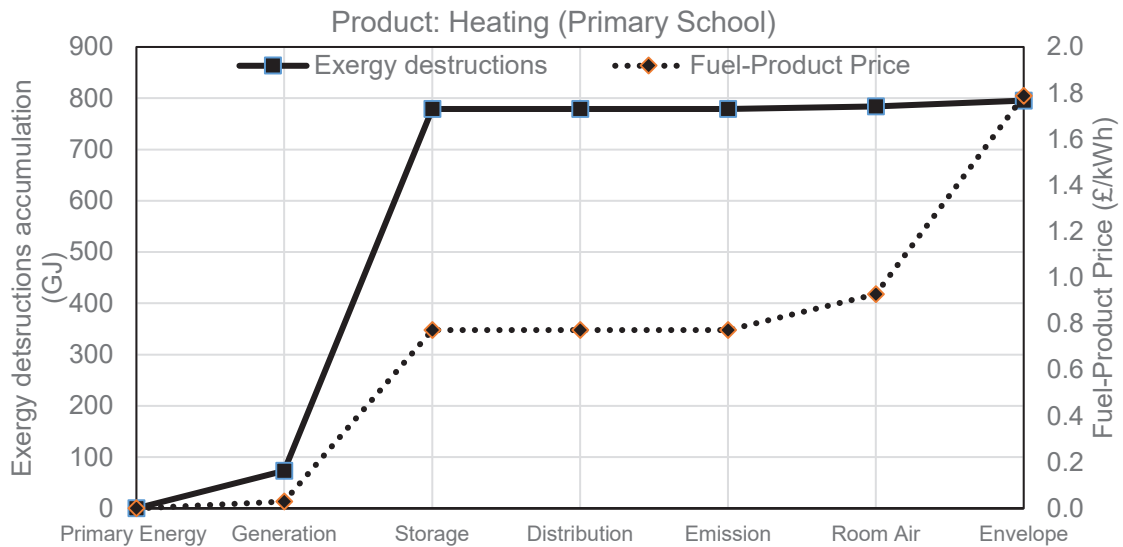
635



636

Fig. 13 Exergy flows by product type. Primary School

637 Fig. 14 illustrates the building heating product cost formation throughout the energy supply
 638 chain, showing that the heating product at the thermal zone increases from £0.03/kWh (gas
 639 price) to £1.79/kWh, with a total relative cost difference r_k of 58.66.



640
 641 **Fig. 14 Exergy destruction accumulation vs product cost formation for the heating stream.**
 642 **Primary School**

643 Until now, as no retrofit strategy has been implemented, no capital cost and revenue can be
 644 calculated ($\dot{Z}_{sys} = 0$, $\dot{R} = 0$). Therefore, the $Exec_{CB,baseline}$ or $\dot{C}_{D,sys}$ has a value of £2.72/h
 645 (£17,672.9/year). By products, exergy destructions cost from heating processes represents
 646 67%, electric appliances 26%, and DHW 7%. The baseline exergy and exergoeconomic values
 647 can be seen in Table 11.

648

| Table 11 Baseline exergy and exergoeconomic values | |
|--|------------------------|
| Baseline characteristics | Primary School |
| Exergy input (fuel) (GJ) | 1915.9 |
| Exergy demand (product) (GJ) | 182.8 |
| Exergy destructions (GJ) | 1733.1 |
| Exergy efficiency HVAC | 1.5% |
| Exergy efficiency DHW | 6.2% |
| Exergy efficiency Electric equip. | 18.0% |
| Exergy efficiency Building | 9.5% |
| Exergy cost fuel-prod HEAT (£/kWh) $\{r_k\}$ | 0.03—1.79 {58.66} |
| Exergy cost fuel-prod COLD (£/kWh) $\{r_k\}$ | ----- {---} |
| Exergy cost fuel-prod DHW (£/kWh) $\{r_k\}$ | 0.03—0.44 {13.66} |
| Exergy cost fuel-prod Elec (£/kWh) $\{r_k\}$ | 0.12—0.26 {1.16} |
| D (£/h) Exergy destructions cost (energy bill £; %D from energy bill) | 2.72 {17,672.9; 90.8%} |
| Z (£/h) Capital cost | 0 |
| Exergoeconomic factor f_k (%) | 1 |
| Exergoeconomic cost-benefit (£/h) | 2.72 |

649 6.2 Optimisation

650 6.2.1 Algorithm settings

651 a) Objective functions

652 As mentioned, an energy optimisation problem requires at least two conflicting problems. In
653 this study three objectives that have to be satisfied simultaneously are going to be investigated.
654 These are the minimisation of overall exergy destructions, reduction of occupant thermal
655 discomfort, and maximisation of project's Net Present Value:

656 I. Building annual exergy destructions (kWh/m²-year):

$$657 Z_1(x) \min = Ex_{dest,bui} = \sum Ex_{prim}(t_k) - \sum Ex_{dem,bui}(t_k) \quad (5)$$

658

659 II. Occupant discomfort hours:

$$660 Z_2(x) \min = (PMV | > 0.5) \quad (6)$$

661

662 III. Net Present Value_{50 years} (£):

$$663 Z_3(x) \max = NPV_{50years} = -TCI + \left(\sum_{n=1}^N \frac{R}{(1+i)^n} \right) + \frac{SV_N}{(1+i)^N} \quad (7)$$

664 However, for simplification and to encode a purely minimisation problem, the NPV is set as
665 negative (although the results will be presented as normal positive outputs). Therefore:

$$666 Z_3(x) \min = -NPV_{50years} = - \left\{ -TCI + \left(\sum_{n=1}^N \frac{R}{(1+i)^n} \right) + \frac{SV_N}{(1+i)^N} \right\} \quad (8)$$

667 b) Constraints

668 Furthermore, it was chosen to subject the optimisation problem to three constraints. First, as
669 a pre-established budget is one of the most common typical limitations in real practice, it was
670 decided to use the initial total capital investment as a constraint. From a previous research
671 [58], a deep retrofit design for this exact same building was suggested with an investment of
672 £734,968.1; therefore, this budget was taken as an economic constraint. In this instance, the
673 aim is to test ExRET-Opt to deliver cheaper solutions with better energetic, exergetic,
674 economic, and thermal comfort performance. Additionally, DPB is also considered as a
675 constraint, sought for solutions with a DPB of 50 years or less, giving positive NPV values.
676 Finally, a third constraint is the maximum baseline discomfort hours, subjecting the model not
677 to worsen the initial baseline conditions (1,443 hours). Hence, the complete optimisation
678 problems can be formulated as follows:

679 Given a ten-dimensional decision variable vector
 680 $x = \{X^{HVAC}, X^{wall}, X^{roof}, X^{ground}, X^{seal}, X^{glaz}, X^{light}, X^{PV}, X^{wind}, X^{heat}\}$, in the solution space X ,
 681 find the vector(s) x^* that:

682
 683 *Minimise:* $Z(x^*) = \{Z_1(x^*), Z_2(x^*), Z_3(x^*)\}$

684 *Subject to follow inequality constraints:* $\begin{cases} TCI \leq \text{£}734,968 \\ DPB \leq 50 \text{ years} \\ Discomfort \leq 1,443 \text{ hrs} \end{cases}$ {constraints}

685
 686 **c) NSGA-II parameters**

687 As GA requires a large population size to efficiently work to define the Pareto front within the
 688 entire search space, Table 12 shows the selected algorithm parameters.

689 **Table 12 Algorithm parameters and stopping criteria for optimisation with GA**

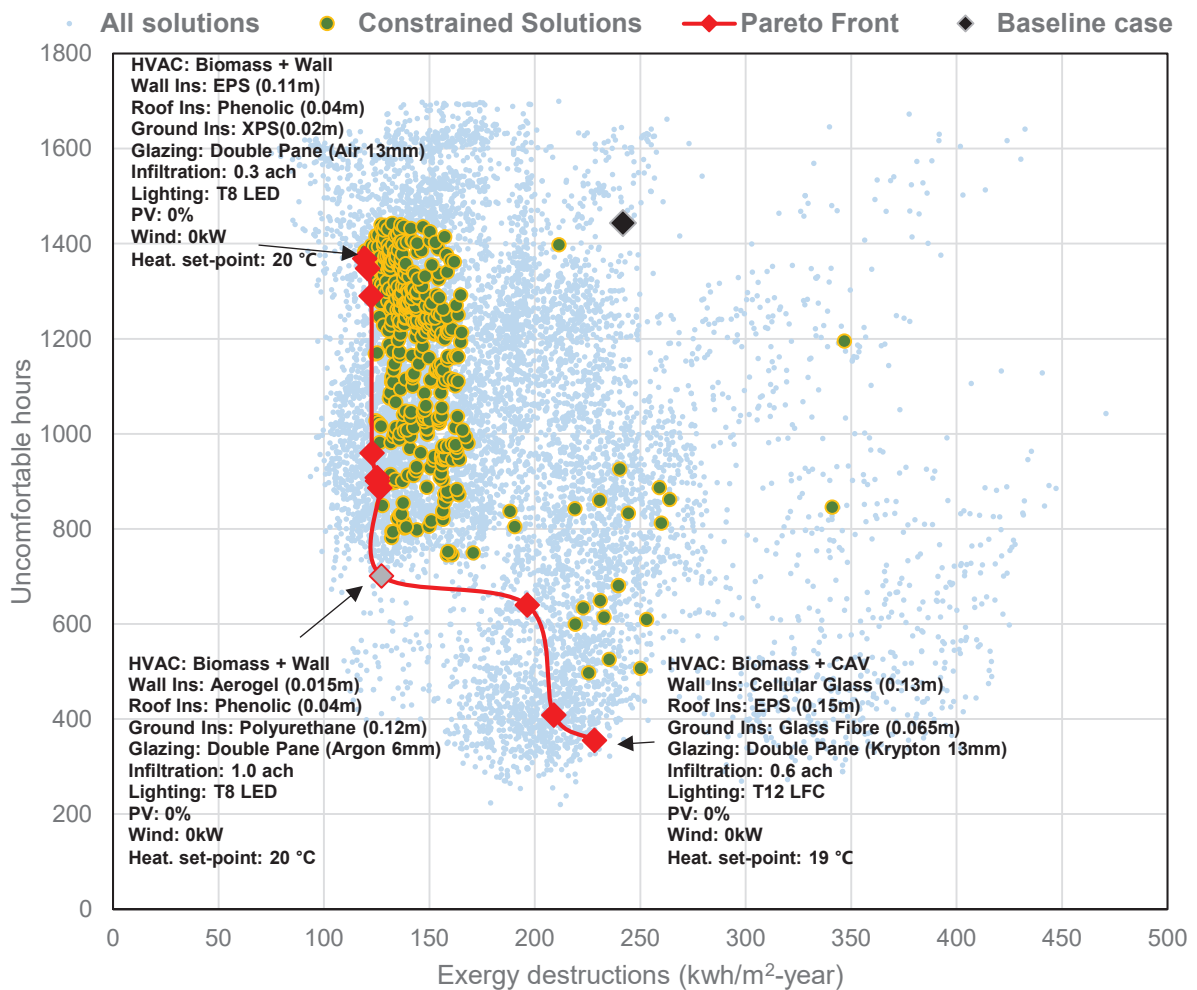
| Parameters | |
|-----------------------------|-----------------------------------|
| <i>Encoding scheme</i> | Integer encoding (discretisation) |
| <i>Population type</i> | Double-Vector |
| <i>Population size</i> | 100 |
| <i>Crossover Rate</i> | 100% |
| <i>Mutation Rate</i> | 20% |
| <i>Selection process</i> | Stochastic – fitness influenced |
| <i>Tournament Selection</i> | 2 |
| <i>Elitism size</i> | Pareto optimal solutions |
| Stopping criteria | |
| <i>Max Generations</i> | 100 |
| <i>Time limit (s)</i> | 10^6 |
| <i>Fitness limit</i> | 10^{-6} |

690
 691 **6.3 Results optimisation**

692
 693 **6.3.1 Dual-objective analysis**

694 In this section, the performance of the system can be presented as a trade-off between the
 695 pairs of objectives to easily illustrate Pareto solutions. This represents an analysis of the three
 696 sets of dual objectives: 1) *Exergy destructions – Comfort*, 2) *Exergy Destruction – NPV*, and
 697 3) *Comfort – NPV*. All simulated solutions, the solutions constrained by the selected criteria,
 698 the baseline case, and the Pareto front are represented in the following graphs. Each solution
 699 in the Pareto front has associated different BER strategies.

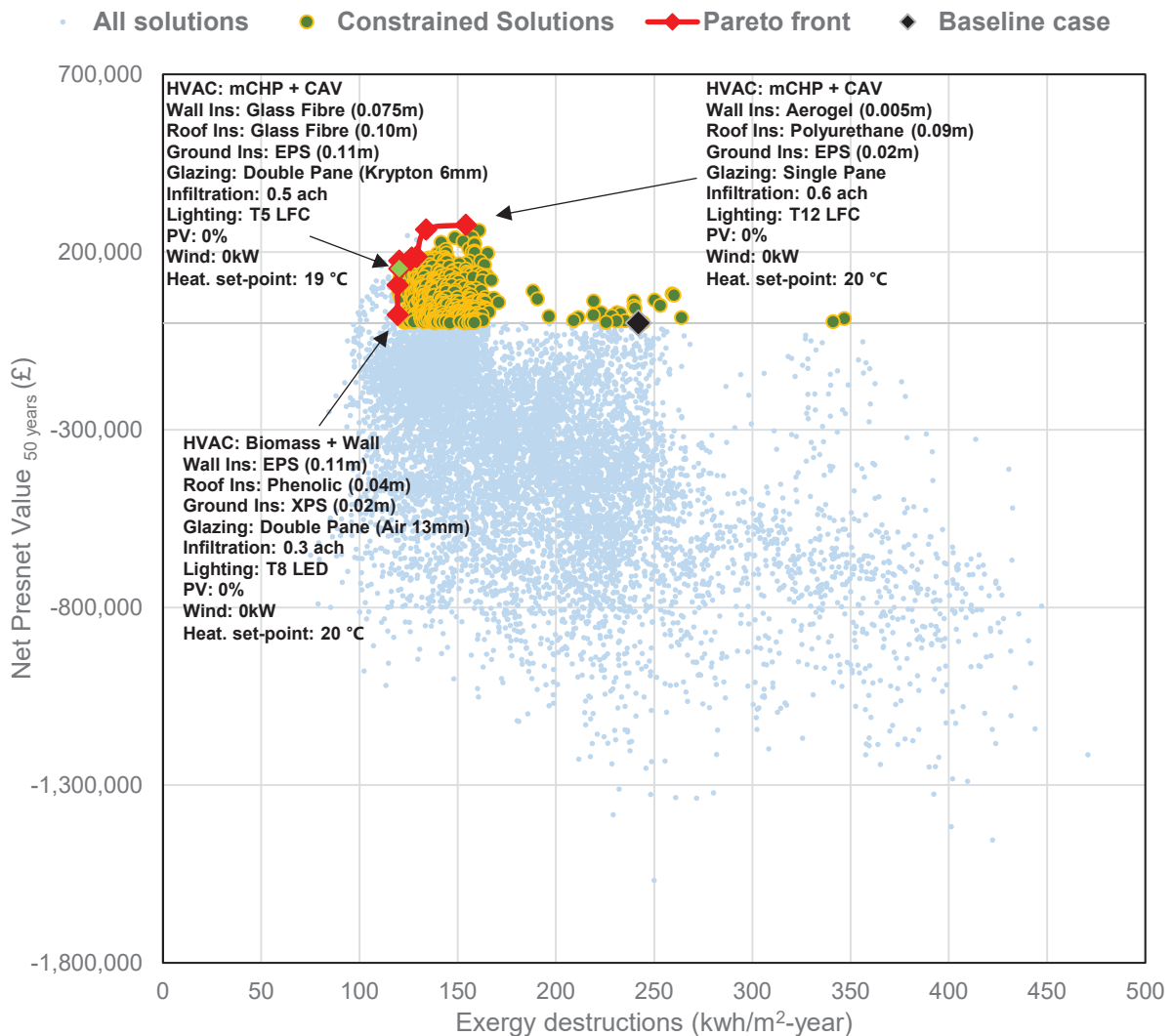
700 Fig. 15 illustrates the simultaneous minimisation of exergy destructions and discomfort hours,
 701 localising the constraint solutions and the Pareto front, formed by eleven designs. Models with
 702 better outputs in the objectives that are not part of the Pareto front are due to the established
 703 constraints, either related to thermal comfort, capital investment, or cost-benefit. When
 704 analysing the Pareto front, the most common HVAC systems are H10: Biomass boiler with
 705 CAV system and H28: Biomass Boiler with wall heating, both with a frequency of 27.3%. For
 706 insulation, no measures with exact technology and thickness repeat; however, the most
 707 common technology is EPS for the wall, Polyurethane and EPS for the roof, and polyurethane
 708 for the ground floor. In respect to the infiltration rate, 0.7 *ach* is the most common value. For
 709 active systems, the T8 LED lighting system, with no PV panels and wind turbines are the most
 710 frequent variables. The minimum value for exergy destructions is achieved by the system H28,
 711 while the minimum value for discomfort by the H10. The whole description of the BER designs
 712 for both optimised extremes can be seen in the graph. Also, the BER design that represents
 713 the model closer to the 'utopia point' is presented. The utopia point is represented by a
 714 theoretical solution that has both optimised values.



715
 716
 717

Fig. 15 Optimisation results and Pareto front (Exergy destructions - Comfort) for the Primary School

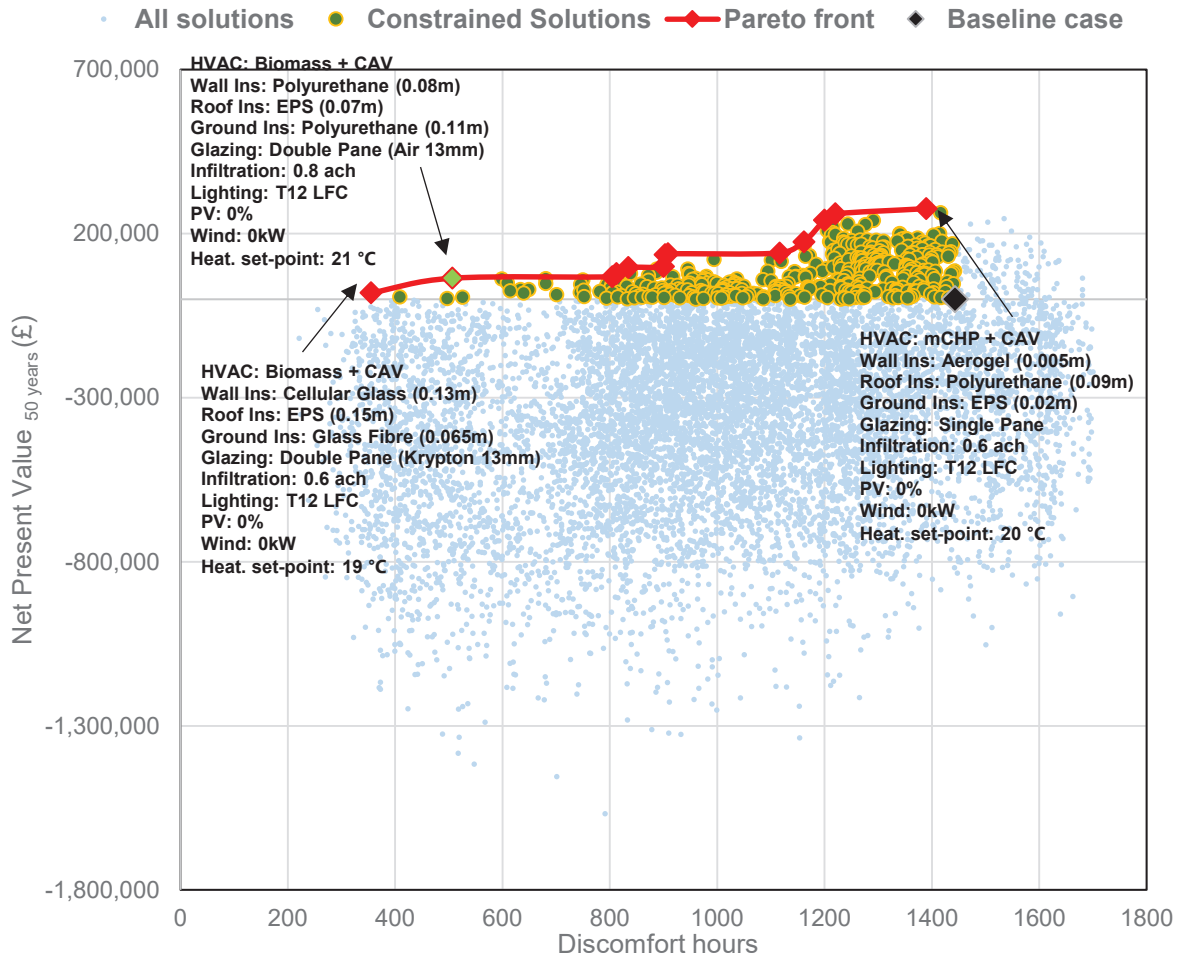
718 Fig. 16 illustrates the simultaneous minimisation of exergy destructions and maximisation of
 719 NPV. In this case, the Pareto front is formed by nine designs. The most frequent HVAC design
 720 is H31: microCHP with a CAV system, presented in eight of the nine cases. The only other
 721 system is H28: Biomass boiler and Wall heating. For the wall insulation, the most frequent
 722 technologies are EPS and glass fibre, while for both roof and ground is EPS. The most
 723 common infiltration rate is 0.4 *ach*, with a frequency of 44.4%, while the most frequent glazing
 724 system (33.3%) is double glazing with 6 mm gap of Krypton. For the lighting system it is T5
 725 LFC, and again no renewable systems are common, where just one of the models includes a
 726 20 kW wind turbine.



727
 728 **Fig. 16 Optimisation results and Pareto front (Exergy destructions - NPV) for the Primary**
 729 **School**

730
 731 The results for the dual optimisation of thermal comfort and NPV are illustrated in Fig. 17. The
 732 Pareto front is formed by thirteen solutions. The most common HVAC system is H28: Biomass
 733 boiler and wall heating with a recurrence of 46.2%. The most common insulation measures

734 are cellular glass and cork board for the walls, EPS for the roof, and polyurethane for the floor.
 735 The infiltration rate that dominates the optimal solutions is 0.8 ach, with no retrofit in the glazing
 736 system. Regarding active systems, the baseline's T12 LFC is the most common solution with
 737 no installation of PV panels and wind turbines.



738
 739 **Fig. 17 Optimisation results and Pareto front (Comfort - NPV) for the Primary School**

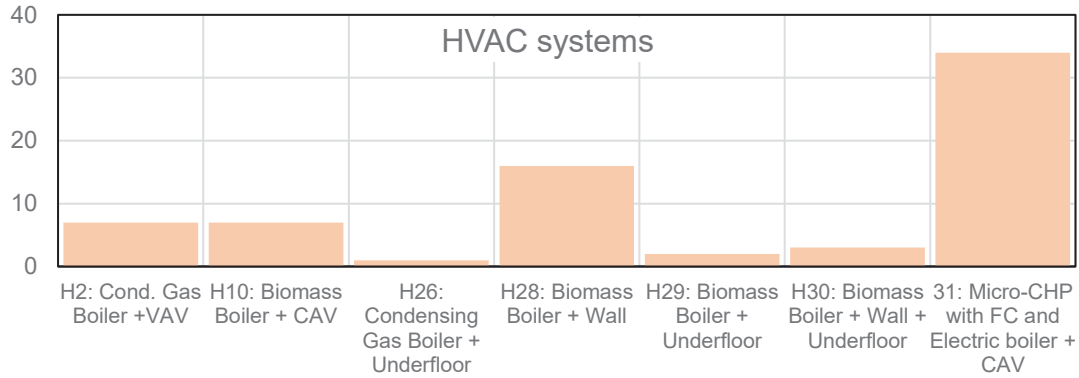
740

741 **6.3.2 Triple-objective analysis**

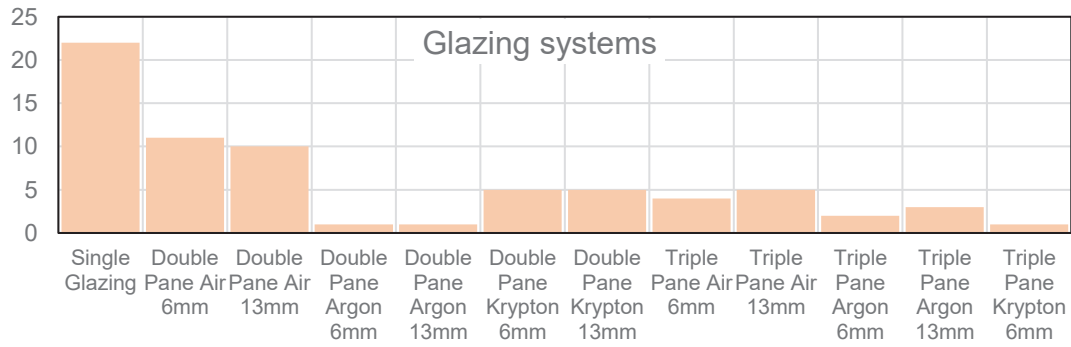
742 The constrained solutions' space consists of 417 models, of which the Pareto surface is
 743 composed of only 70 possible solutions. Given the constraints, the Pareto results suggest that
 744 the optimisation study found more models oriented to minimise exergy destructions and
 745 maximise NPV, while struggling to optimise the thermal comfort objective. This is also
 746 complemented by the fact that the majority of optimal solutions present high values of
 747 infiltration levels ($0.5 < x < 1.0$ ach). This might be the case for obtaining average improvement
 748 in occupant thermal comfort. Nevertheless, the Pareto front also obtained models with good
 749 thermal comfort performance, with discomfort values of 400 hours or less annually. Regarding
 750 the HVAC system, H31: mCHP with CAV system is presented in the majority of optimal

751 solutions. On the other hand, the optimisation suggests not to retrofit the glazing systems due
 752 to its high capital investment costs. In respect to insulation, Polyurethane is found to be the
 753 most frequent technology among all three parts of the envelope. The most common insulation
 754 thicknesses are found to be 5 cm, 1cm, and 2 cm for wall, roof, and ground respectively. Fig.
 755 18 shows the frequency distribution of the main BER solutions in the Pareto front.

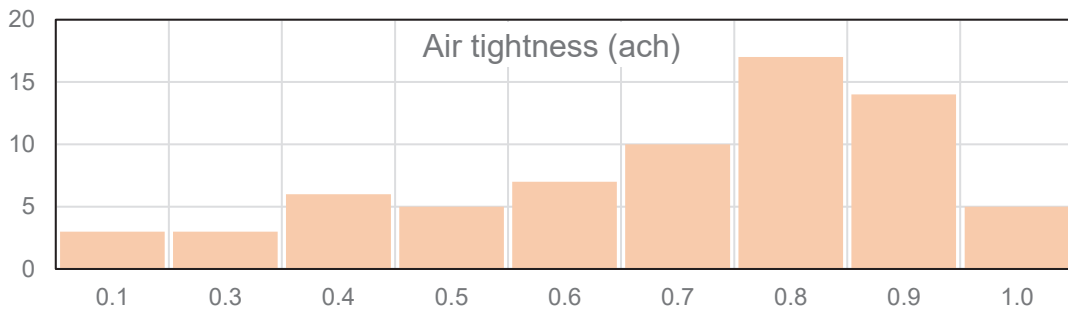
756



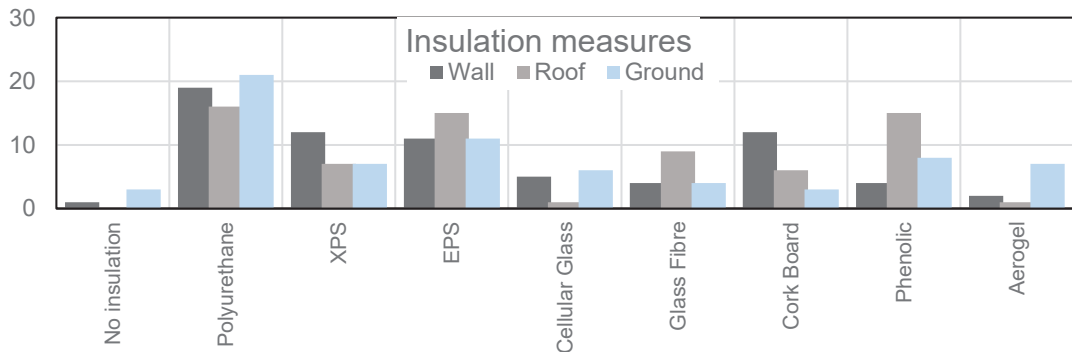
757



758



759



760
761

Fig. 18 Frequency distribution graphs of main retrofit variables from the Pareto front for the Primary School case study

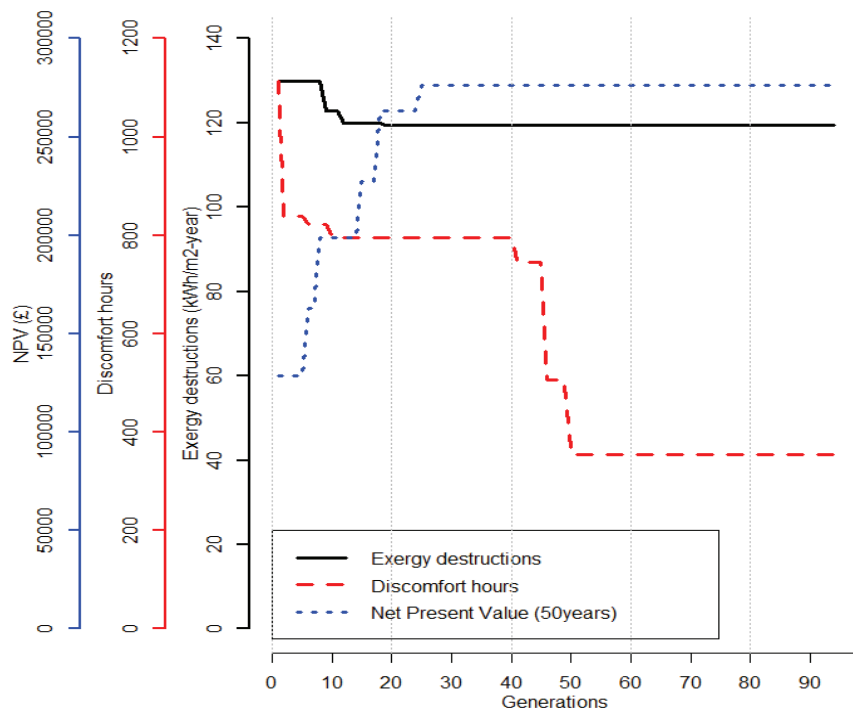
762 Other design variables that are not illustrated and dominate the Pareto front are T12 LFC for
 763 the lighting system, the implementation of a 20 kW wind turbine, lack of installation of PV roof
 764 panels, and a heating set-point of 18 °C. This set-point variable also impacts the poor
 765 improvement in thermal comfort.

766

767 **6.3.3 Algorithm behaviour - Convergence study**

768 For both cases, the convergence metrics were computed for every generation. Fig. 19
 769 illustrates the evolution of the three objective functions corresponding to each generation and
 770 its convergence with an allowance of one hundred generations. The results demonstrate that
 771 exergy destructions converged after the nineteenth generation (119.4 kWh/m²-year),
 772 discomfort hours converged after the fiftieth (355 hours), and NPV after the twenty-fifth
 773 generation (£276,182). As it can be seen, the minimum value for exergy destructions found in
 774 the first generation (129.8 kWh/m²-year) is similar to the one found in the last generations,
 775 meaning that the algorithm selected a ‘strong’ and ‘healthy individual’ (building model) from
 776 the first generation. However, due to the model’s strict constraints, larger number of
 777 generations are required for the discomfort hours to converge within an acceptable value.

778



779

780 **Fig. 19 Convergence of Primary School optimisation procedure for the three objective**
 781 **functions**

782

783 *6.4 Multiple-criteria decision analysis (compromise programming)*

784 In order to tackle the multi-objective optimisation procedure within ExRET-Opt, the MCDM
 785 module is used. In compromise programming, firstly, the non-dominated set is defined with
 786 respect to the ideal (Utopian - Z^*) and anti-ideal (Nadir - Z_*) points, which represent the
 787 optimisation and anti-optimisation of each objective individually. For this study, the process
 788 can be written as follows:

$$789 \quad \alpha_{exergy_dest} \geq \left(\frac{|Z_{exergy_dest}(x) - Z^*_{exergy_dest}|}{|Z^*_{exergy_dest} - Z_*_{exergy_dest}|} \right) * (p_{exergy_dest}) \quad (9)$$

$$790 \quad \alpha_{discomfort} \geq \left(\frac{|Z_{discomfort}(x) - Z^*_{discomfort}|}{|Z^*_{discomfort} - Z_*_{discomfort}|} \right) * (p_{discomfort}) \quad (10)$$

$$791 \quad \alpha_{NPV} \geq \left(\frac{|Z^*_{NPV} - Z_{NPV}(x)|}{|Z^*_{NPV} - Z_*_{NPV}|} \right) * (p_{NPV}) \quad (11)$$

792 For the application of compromise programming, the weighting procedure by scanning different
 793 combinations for the three objectives is subject to the following constraint:

$$794 \quad \sum_{j=1}^n p_j = p_{exergy_dest} + p_{discomfort} + p_{NPV} = 1 \quad (12)$$

795

796 Finally, as an individual distance (α_j) is obtained for each objective, these are added up for
 797 every solution:

$$798 \quad \alpha_{cheb} = \sum_{j=1}^n \alpha_j = \alpha_{exergy_dest} + \alpha_{discomfort} + \alpha_{NPV} \geq 0 \quad (13)$$

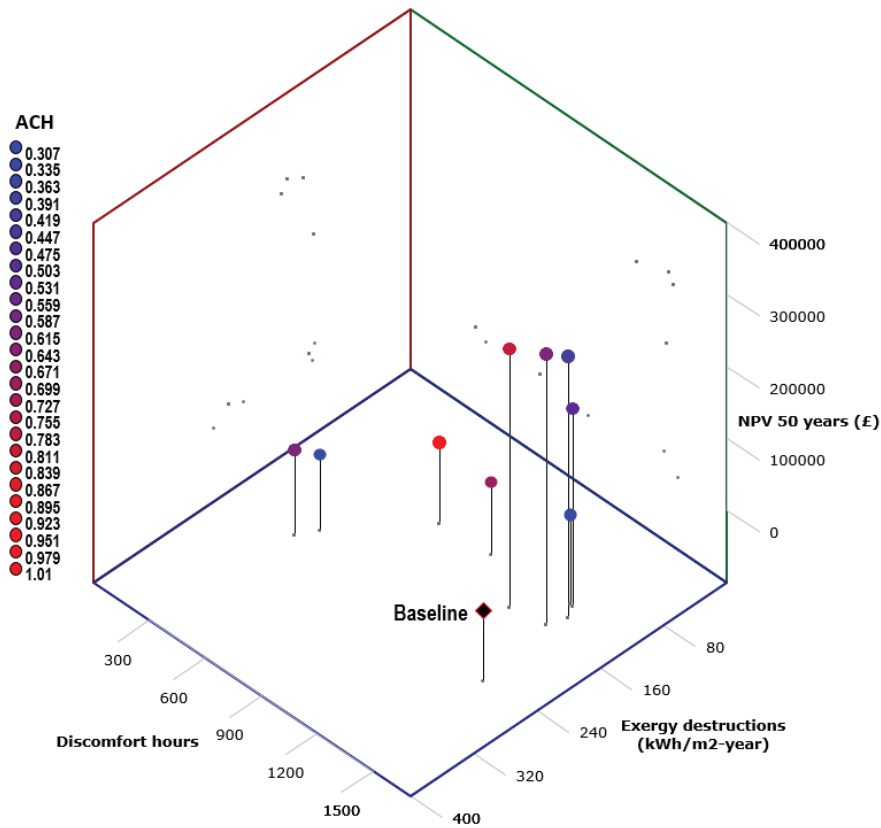
799

800 The method then scans all the feasible sets and minimises the deviation from the ideal point,
 801 obtaining the minimum Chebyshev distance ($[\min]\alpha_{cheb}$):

$$802 \quad [\min]\alpha_{cheb} = \min \sum_{j=1}^n \alpha_j \quad (14)$$

803

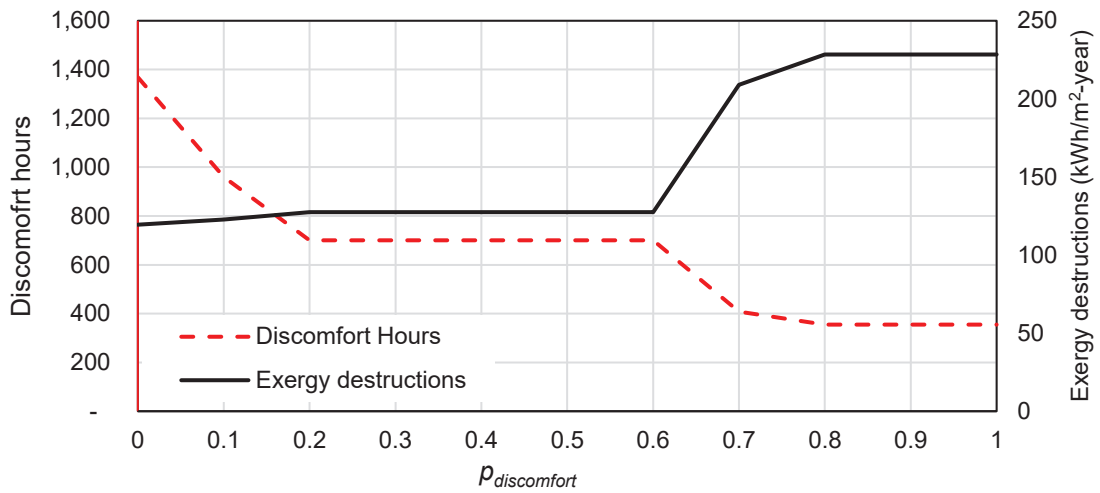
804 For the case study, the entire range of defined criteria and different weights of coefficient
 805 values is summarised in Appendix B. The table shows the best solution for each weighting
 806 design showing the BER retrofit parameters code (Appendix A) along the obtained results for
 807 each objective function. Having this type of information gives the decision maker the flexibility
 808 and possibility of a straightforward BER design change, if new insights arise as a result of the
 809 objectives' priorities adjustment. From a detailed analysis of the outputs, it is found that only
 810 nine solutions are considered by the MCDM, as similar BER design repeats in different
 811 weighting coefficients (Fig. 20).



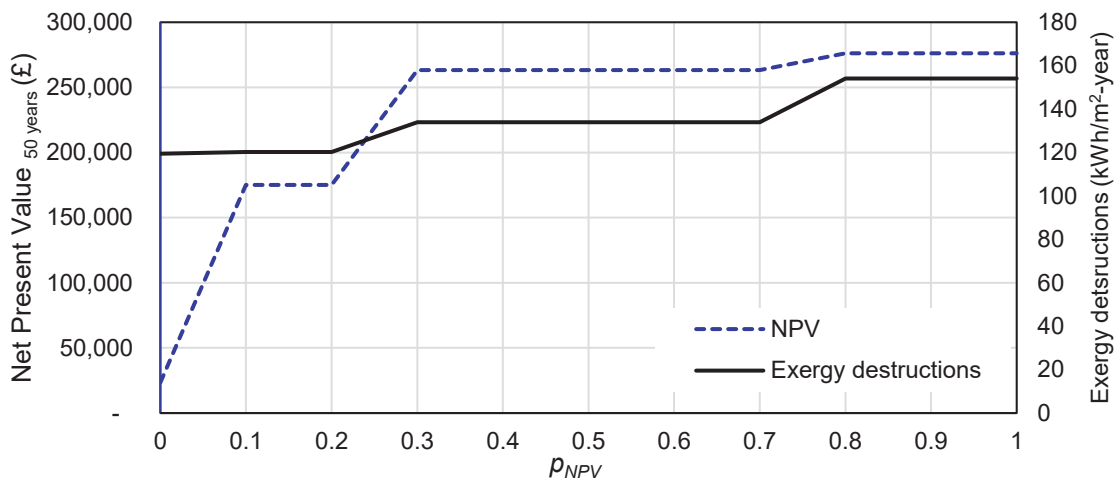
812
813
814

Fig. 20 Primary School optimal solutions found by Compromise Programming MCDM method

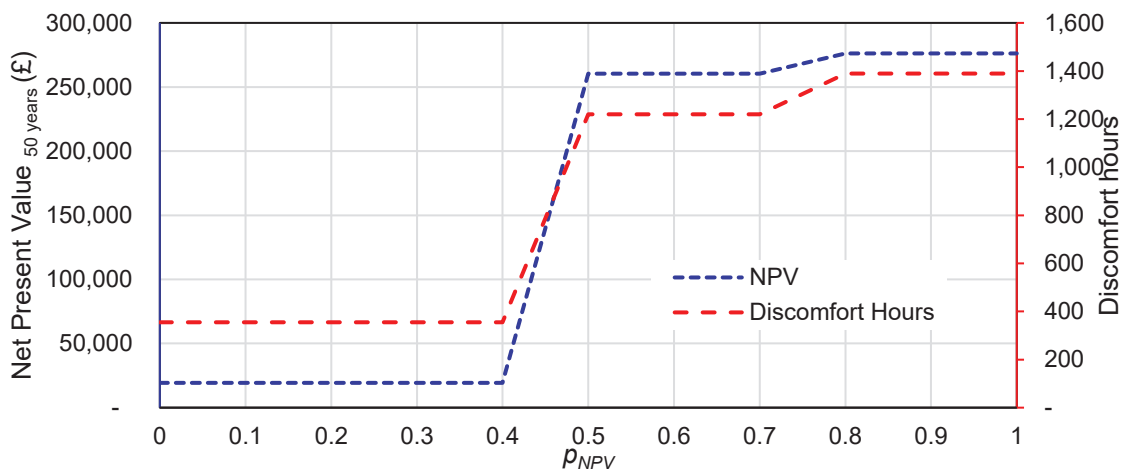
815 Fig. 21 shows the compromise solutions for different weights for all pairs of objective functions
 816 combinations, demonstrating how the objective functions' outputs change with respect to the
 817 coefficient weight. These graphs show the competitive nature of all three objectives. For
 818 example, as a result of demanding more exergy to cover internal thermal conditions, an
 819 increase in exergy destructions leads to a decrease in occupant thermal discomfort. However,
 820 meeting at $p_{exergy}=0.4$ and $p_{discomfort}=0.6$ good solutions for both objectives can be obtained.
 821 When comparing NPV and exergy destructions, it demonstrates that projects with higher NPV
 822 merely increase exergy destructions, meaning that a compromise in building exergy efficiency
 823 could lead to a more profitable project. Finally, a less profitable project (low NPV) is required
 824 to obtain good internal conditions as a result of two reasons: the necessity of more energy
 825 leading to a larger expenditure and/or the need to have a higher capital investment for
 826 technology that leads to better internal conditions.



827



828



829

830 Fig. 21 Changes in the Primary School objective function values with respect to the weighting coefficient

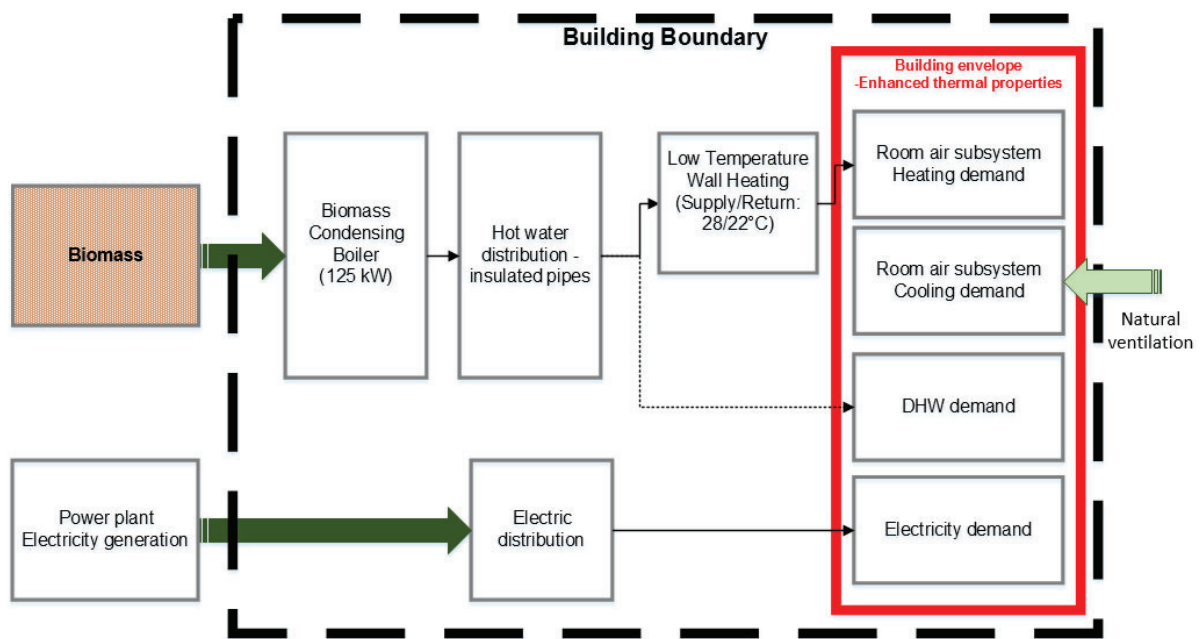
831

832 6.5 Utopian solution vs baseline case

833 For a final comparison, the utopian solution is selected. The utopia point is a theoretical model
 834 which contains the minimum value for each of the three objectives optimised individually. To
 835 find this particular model, a weight coefficient with similar values has to be considered
 836 ($p_{exergy_dest}=0.33$, $p_{discomfort}=0.33$, and $p_{NPV}=0.33$).

837 For the case study, the retrofitted model close to the utopia consists of an HVAC system H28:
 838 a 125 kW biomass-based condensing boiler connected to a low temperature wall heating
 839 system working with a heating set-point at 20 °C. The insulation for the wall is composed of
 840 Aerogel with a thickness of 0.015m, while the roof insulation is composed of 0.04m of phenolic
 841 board, and the ground of 0.12m of polyurethane. The infiltration rate keeps the baseline levels
 842 of 1.0 *ach*, while the glazing system is retrofitted with double-glazed, with a 6mm gap of Argon
 843 gas. For active systems, the lighting system is retrofitted to install T8 LEDs. Furthermore, the
 844 BER design does not consider any implementation of renewable electricity generation (PV or
 845 wind turbines). A schematic diagram of the building energy system in Fig. 22.

846



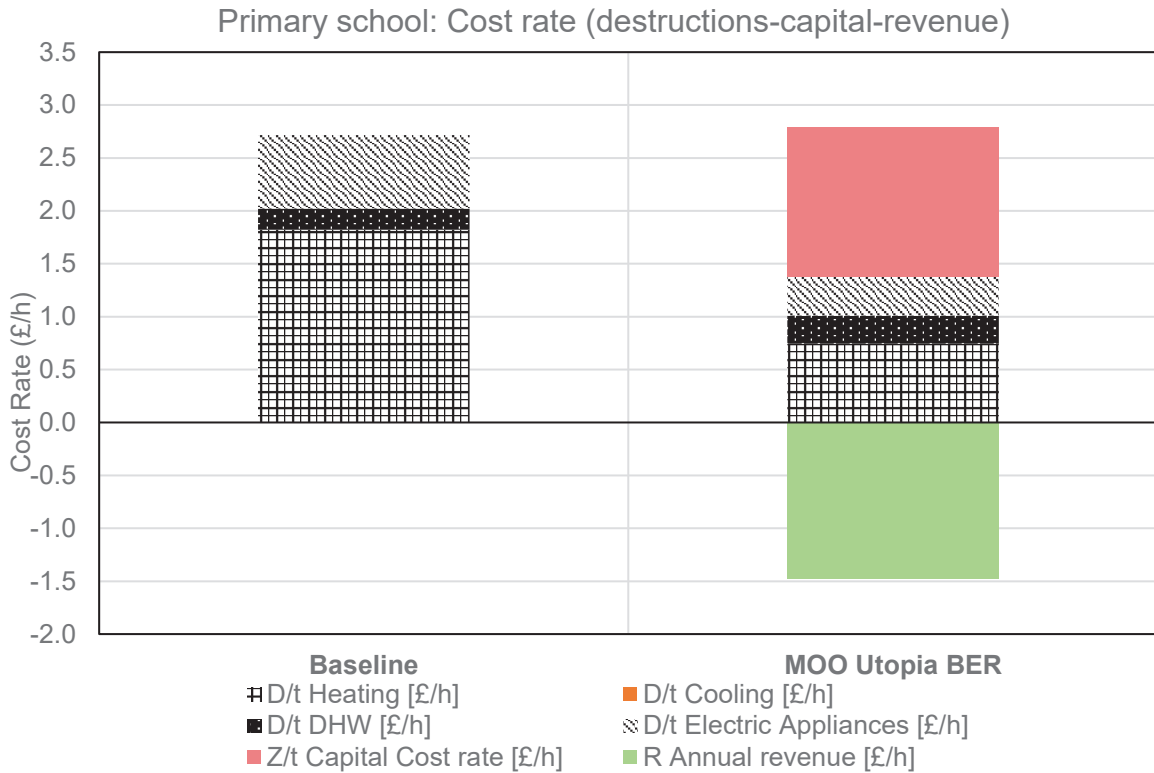
847

848 **Fig. 22 Schematic layout of the energy system for the Primary School 'close to Utopia' BER**
 849 **model**

850 From the baseline value of 187.9 kWh/m²-year for energy use, the utopian model reduces it to
 851 118.1 kWh/m²-year. The utopian model compromises on greater energy use savings, as the
 852 optimisation process has a constraint to achieve a DPB of 50 years or less with a maximum
 853 budget of £734,968. This utopian model requires a retrofit capital cost of just £329,856,
 854 achieving a DPB of 49 years. Nevertheless, the utopian model improves on thermal comfort
 855 levels from a baseline value of 1,443 uncomfortable hours to 701 hours for the post-retrofit
 856 building. Additionally, the optimised design was able to reduce carbon emission baseline value
 857 up to 72.8%.

858 Notwithstanding, interesting outputs come from the exergy and exergoeconomic analyses. Fig.
 859 23, showing that total exergy destruction rates are £1.38/h for the utopian model; representing
 860 a major improvement from the baseline case (£2.7/h). Moreover, BER capital cost rate - **Z** (in
 861 light red) and annual revenue rate - **R** (in light green) are illustrated for the utopian model. The

862 utopian model achieves a Z of £1.41/h and an R of £1.47/h. When analysing the $Exec_{CB}$
 863 indicator with the aim to find the best possible exergoeconomic design, this results in a value
 864 of £1.31/h, meaning that the obtained design provides better overall exergy/exergoeconomic
 865 performance compared to the pre-retrofitted building.
 866



867
 868 **Fig. 23 Primary school exergy destruction, BER capital cost and annual revenue cost rate**

869 The framework developed in this research has demonstrated to provide designs with an
 870 appropriate balance between active and passive measures, while consistently accounting for
 871 energy use, irreversibilities, and exergetic and economic costs along every subsystem in the
 872 building energy system. Meanwhile, the application of the exergoeconomic cost-benefit index
 873 could be a practical solution to supports building designers in making informed and robust
 874 economic decisions.

875 **7. Conclusions**

876 This paper presented ExRET-Opt, a retrofit-oriented simulation framework, which has become
 877 a part of EnergyPlus in performing exergy and exergoeconomic balances. The addition was
 878 done thanks to the development of external Python-based subroutines, and the support of the
 879 Java-based software jEPlus. ExRET-Opt, apart from providing the user with exergy data and
 880 pinpointing sources of inefficiencies along the energy supply chain, gives the possibility to
 881 perform a comprehensive exploration of a wide range state-of-the-art building energy
 882 technologies, with the intention to minimise energy use and improve thermodynamic efficiency

883 of existing buildings. The retrofit technologies include high and low temperature HVAC
884 systems, envelope insulation measures, insulated glazing systems, efficient lighting, energy
885 renewable generation technologies, and set-points control measures. Moreover, integration of
886 exergoeconomic analysis and multi-objective optimisation into EnergyPlus allows users to
887 perform a comprehensive exergoeconomic optimisation similar to those found in the
888 optimisation of chemical or power generation processes. It means that indicators such as
889 energy, exergy, economic (capital cost, NPV), exergoeconomic, and carbon emissions
890 combined with occupants' thermal comfort, can be used as constraints or objective functions
891 in the optimisation procedure. The limited availability of robust and comprehensive test data
892 has restricted the application of full validation tests to the results of ExRET-Opt. However, an
893 inter-model and analytical verification processes was performed. By reviewing different
894 existing exergy tools and exergy-based research, the calculation process of the two main
895 subroutines developed for ExRET-opt, has been verified with acceptable results.

896 To demonstrate the strengths of ExRET-Opt in a real case study, the framework was applied
897 to a school building. A hybrid-thermodynamic MOO problem, considering net present value
898 (First Law), exergy destructions (Second Law), and occupant thermal comfort as objective
899 functions was performed. Outputs demonstrate that by using exergy and NPV as objective
900 functions it is possible to improve energy and exergy performance, reduce carbon and exergy
901 destructions footprint, while also providing comfortable conditions under cost-effective
902 solutions. This gives practitioners and decision makers more flexibility in the design process.
903 Additionally, the results show that even with the imposed constraints, the NSGA-II-based MOO
904 module was successfully applied, finding a large range of better performance BER designs for
905 the analysed case study, compared with their corresponding baseline case. However, a tight
906 (constrained) budget means missing out on some low-exergy systems, which require higher
907 capital investment, such as district heating/cooling systems and ground source heat pumps.
908 Finally, to compare the strength of an exergy-based MOO-MCDM, the utopian model was
909 selected for a final comparison against the pre-retrofitted case. This solution represents the
910 model closest to the optimal objectives, if they were optimised separately. These final selected
911 solutions improved overall building's energy performance, exergy efficiency and buildings' life
912 cycle cost while having low initial capital investments.

913 It is suggested that BER designs should result from a more holistic analysis. Exergy and
914 exergoeconomics could have an important future role in the building industry if some practical
915 barriers were overcome. The proposed methodological framework can provide more
916 information than the typical optimisation methods based solely on energy analysis. The
917 addition of exergy/exergoeconomic analysis to building optimisation completes a powerful and
918 robust methodology that should be pursued in everyday BER practice. By utilising popular
919 buildings' simulation tools as the foundation, practical exergy and exergoeconomics theory
920 could become more accessible, reaching a wider audience of industry decision makers as well

921 as academic researchers. Combined with other methods, such as multi-objective optimisation
 922 and multi criteria decision making, exergy finally could hold a good chance to find a place in
 923 the everyday practice.

924 **Acknowledgments**

925 The first author acknowledges support from The Mexican National Council for Science and
 926 Technology (CONACyT) through a scholarship to pursue doctoral studies with a CVU: 331698
 927 and grant number: 217593.

928 **Nomenclature**

| | | |
|-----|----------------------|---|
| 929 | BER | building energy retrofit |
| 930 | \dot{C}_D | exergy destruction cost (£) |
| 931 | c_f | average cost of fuel (£/kWh) |
| 932 | c_p | average cost of product (£/kWh) |
| 933 | DPB | discounted payback (years) |
| 934 | EUI | energy use index (kWh/m ² -year) |
| 935 | Ex | exergy (kWh) |
| 936 | $\dot{E}x_D$ | exergy destructions (kWh) |
| 937 | Exe_{CB} | exergoeconomic cost benefit factor (£/h) |
| 938 | f_k | exergoeconomic factor (-) |
| 939 | NPV | net present value (£) |
| 940 | R | annual revenue (£) |
| 941 | TCI | total capital investment (£) |
| 942 | \dot{Z}_k | capital investment rate (£/h) |
| 943 | Greek symbols | |
| 944 | α_{cheb} | Chebyshev distance |
| 945 | ψ_{tot} | exergy efficiency (-) |

946 **Appendix A. Characteristics of building retrofit measures [58]**

947 **Table A.1 Characteristics and investment cost of HVAC systems**

| HVAC ID | System Description | Emission system | Cost |
|---------|---|-----------------|---|
| H1 | Condensing Gas Boiler + Chiller | CAV | <i>Generation systems</i> • £160/kW Water-based Chiller (COP=3.2) • £99/kW Condensing gas boiler ($\eta=0.95$) • £70/kW Oil Boiler ($\eta=0.90$) • £150/kW Electric Boiler ($\eta=1.0$) |
| H2 | Condensing Gas Boiler + Chiller | VAV | |
| H3 | Condensing Gas Boiler + ASHP-VRF System | FC | |
| H4 | Oil Boiler + Chiller | CAV | |
| H5 | Oil Boiler + Chiller | VAV | |
| H6 | Oil Boiler + Chiller | FC | |
| H7 | Electric Boiler + Chiller | CAV | |
| H8 | Electric Boiler + Chiller | VAV | |

| | | | |
|-----|--|-----------------|--|
| H9 | <i>Electric Boiler + ASHP-VRF System</i> | FC | • £208/kW Biomass Boiler ($\eta=0.90$) |
| H10 | <i>Biomass Boiler + Chiller</i> | CAV | • £1300/kW ASHP-VRF System (COP=3.2) |
| H11 | <i>Biomass Boiler + Chiller</i> | VAV | • £1200/kW GSHP (Water-Water) System (COP=4.2) |
| H12 | <i>Biomass Boiler + ASHP-VRF System</i> | FC | • £452/kW ASHP (Air-Air) (COP=3.2) |
| H13 | <i>District system</i> | CAV | • £2000/kW PV-T system |
| H14 | <i>District system</i> | VAV | • £27,080 micro-CHP (5.5 kW) + fuel cell system |
| H15 | <i>District system</i> | Wall | |
| H16 | <i>District system</i> | Underfloor | |
| H17 | <i>District system</i> | Wall+Underfloor | |
| H18 | <i>Ground Source Heat Pump</i> | CAV | |
| H19 | <i>Ground Source Heat Pump</i> | VAV | |
| H20 | <i>Ground Source Heat Pump</i> | Wall | Emission systems |
| H21 | <i>Ground Source Heat Pump</i> | Underfloor | • £700 per CAV |
| H22 | <i>Ground Source Heat Pump</i> | Wall+Underfloor | • £1200 per VAV |
| H23 | <i>Air Source Heat Pump</i> | CAV | • £35/m ² wall heating |
| H24 | <i>PVT-based system (50% roof) with supplemental Electric boiler and Old Chiller</i> | CAV | • £35/m ² underfloor heating |
| H25 | <i>Condensing Boiler + Chiller</i> | Wall | • £6117 per Heat Recovery system |
| H26 | <i>Condensing Boiler + Chiller</i> | Underfloor | |
| H27 | <i>Condensing Boiler + Chiller</i> | Wall+Underfloor | Other subsystems: |
| H28 | <i>Biomass Boiler + Chiller</i> | Wall | • £56/kW District heat exchanger + £6122 connection charge |
| H29 | <i>Biomass Boiler + Chiller</i> | Underfloor | |
| H30 | <i>Biomass Boiler + Chiller</i> | Wall+Underfloor | • £50/m for building's insulated distribution pipes |
| H31 | <i>Micro-CHP with Fuel Cell and Electric boiler and old Chiller</i> | CAV | |
| H32 | <i>Condensing Gas Boiler and old Chiller. Heat Recovery System included.</i> | CAV | |

948
949

Table A.2 Characteristics and investment cost of lighting systems

| Lights ID | Lighting technology | Cost per W/m ² |
|-----------|---------------------|---------------------------|
| L1 | T8 LFC | £5.55 |
| L2 | T5 LFC | £7.55 |
| L3 | T8 LED | £11.87 |

950

Table A.3 Characteristics and investment cost of renewable energy generation systems

| Renewable | Technology | Cost |
|-----------|--------------------|--------------------------|
| R1 | PV panels 25% roof | PV: £1200/m ² |
| R2 | PV panels 50% roof | |
| R3 | PV panels 75% roof | |
| R4 | Wind Turbine 20 kW | Turbine: £4000/kW |
| R5 | Wind Turbine 40 kW | £/kW |

952

Table A.4 Characteristics and investment cost of different insulation materials

| Ins. ID | Insulation measure | Thickness (cm) | Total of measures | Cost per m ² (lowest to highest) |
|---------|-----------------------------|-----------------------|-------------------|---|
| I1 | <i>Polyurethane</i> | 2 to 15 in 1 cm steps | 14 | £6.67 to £23.32 |
| I2 | <i>Extruded polystyrene</i> | 1 to 15 in 1 cm steps | 15 | £4.77 to £31.99 |
| I3 | <i>Expanded polystyrene</i> | 2 to 15 in 1 cm steps | 14 | £4.35 to £9.95 |
| I4 | <i>Cellular Glass</i> | 4 to 18 in 1 cm steps | 15 | £16.21 to £72.94 |

953

| | | | | |
|----|----------------------------|--|----|-------------------|
| 15 | <i>Glass Fibre</i> | 6.7, 7.5, 8.5, and 10 cm | 4 | £5.65 to £7.75 |
| 16 | <i>Cork board</i> | 2 to 6 in 1 cm steps, 8 to 20 cm in 2 cm steps, 28 and 30 cm | 14 | £5.57 to £85.80 |
| 17 | <i>Phenolic foam board</i> | 2 to 10 in 1 cm steps | 9 | £5.58 to £21.89 |
| 18 | <i>Aerogel</i> | 0.5 to 4 in 0.5 cm steps | 8 | £26.80 to £195.14 |
| 19 | <i>PCM (w/board)</i> | 10 and 20 mm | 2 | £57.75 to £107.75 |

954

955

Table A.5 Characteristics and investment cost of glazing systems

| Glazing ID | System Description (# panes – gap) | Gas Filling | Cost per m² |
|-------------------|---|--------------------|-------------------------------|
| G1 | <i>Double pane - 6mm</i> | Air | £261 |
| G2 | <i>Double pane - 13mm</i> | Air | £261 |
| G3 | <i>Double pane - 6mm</i> | Argon | £350 |
| G4 | <i>Double pane - 13mm</i> | Argon | £350 |
| G5 | <i>Double pane - 6mm</i> | Krypton | £370 |
| G6 | <i>Double pane - 13mm</i> | Krypton | £370 |
| G7 | <i>Triple pane - 6mm</i> | Air | £467 |
| G8 | <i>Triple pane - 13mm</i> | Air | £467 |
| G9 | <i>Triple pane - 6mm</i> | Argon | £613 |
| G10 | <i>Triple pane - 13mm</i> | Argon | £613 |
| G11 | <i>Triple pane - 6mm</i> | Krypton | £653 |
| G12 | <i>Triple pane - 13mm</i> | Krypton | £653 |

956

957

958

Table A.6 Characteristics and investment cost for air tightness improvement considering baseline of 1 ach

| Sealing ID | ACH (1/h) Improvement % | Cost per m² (opaque envelope) |
|-------------------|--------------------------------|---|
| S1 | 10% | £1.20 |
| S2 | 20% | £3.31 |
| S3 | 30% | £6.35 |
| S4 | 40% | £10.30 |
| S5 | 50% | £15.20 |
| S6 | 60% | £20.98 |
| S7 | 70% | £27.69 |
| S8 | 80% | £35.33 |
| S9 | 90% | £43.88 |

959

960

Table A.7 Cooling and heating indoor set points variations

| Set-point ID | Set-point Type | Value (°C) | Cost |
|---------------------|-----------------------|-------------------|-------------|
| SH18 | <i>Heating</i> | 18 | (-) |
| SH19 | | 19 | |
| SH20 | | 20 | |
| SH21 | | 21 | |
| SH22 | | 22 | |
| SC23 | <i>Cooling</i> | 23 | (-) |
| SC24 | | 24 | |
| SC25 | | 25 | |
| SC26 | | 26 | |
| SC27 | | 27 | |

961

962 Appendix B. Multi-criteria decision making outputs

963
964

Table B-1 Sample of 'optimal solutions' obtained from Primary School Pareto front using Compromise Programming

| p_{ex} | p_{com} | p_{NPV} | α_{cheb} [min] | $Ex_{dest,bui}$ (kWh/m ² -year) | Discomfort (hours) | $NPV_{50years}$ (£) | X^{HVAC} (Type) | X^{wall} (m) | X^{roof} (m) | X^{ground} (m) | X^{seal} (ach) | X^{glaz} (type) | X^{light} Light techn. | X^{PV} % roof panels | X^{wind} (kW) | X^{heat} (°C) |
|----------|-----------|-----------|-----------------------|--|--------------------|---------------------|-------------------|----------------|----------------|------------------|------------------|-------------------|--------------------------|------------------------|-----------------|-----------------|
| 1 | 0 | 0 | 0.00 | 119.4 | 1,369 | 23,493 | 28 | 3.11 | 7.04 | 2.02 | 0.3 | 2 | 3 | 0 | 0 | 20 |
| 0.9 | 0.1 | 0 | 0.08 | 122.8 | 960 | 2,069 | 28 | 3.02 | 4.05 | 4.12 | 0.7 | 1 | 3 | 0 | 20 | 19 |
| 0.9 | 0 | 0.1 | 0.04 | 120.3 | 1,382 | 175,127 | 31 | 5.075 | 5.1 | 3.11 | 0.5 | 5 | 2 | 0 | 0 | 19 |
| 0.8 | 0.2 | 0 | 0.11 | 127.4 | 701 | 13,964 | 28 | 8.015 | 7.04 | 1.12 | 1 | 3 | 3 | 0 | 0 | 20 |
| 0.8 | 0.1 | 0.1 | 0.14 | 120.3 | 1,382 | 175,127 | 31 | 5.075 | 5.1 | 3.11 | 0.5 | 5 | 2 | 0 | 0 | 19 |
| 0.8 | 0 | 0.2 | 0.08 | 120.3 | 1,382 | 175,127 | 31 | 5.075 | 5.1 | 3.11 | 0.5 | 5 | 2 | 0 | 0 | 19 |
| 0.7 | 0.3 | 0 | 0.14 | 127.4 | 701 | 13,964 | 28 | 8.015 | 7.04 | 1.12 | 1 | 3 | 3 | 0 | 0 | 20 |
| 0.7 | 0.2 | 0.1 | 0.20 | 127.4 | 701 | 13,964 | 28 | 8.015 | 7.04 | 1.12 | 1 | 3 | 3 | 0 | 0 | 20 |
| 0.7 | 0.1 | 0.2 | 0.17 | 120.3 | 1,382 | 175,127 | 31 | 5.075 | 5.1 | 3.11 | 0.5 | 5 | 2 | 0 | 0 | 19 |
| 0.7 | 0 | 0.3 | 0.09 | 134.0 | 1,417 | 263,272 | 31 | 3.14 | 3.15 | 1.11 | 0.4 | 0 | 0 | 0 | 0 | 20 |
| 0.6 | 0.4 | 0 | 0.16 | 127.4 | 701 | 13,964 | 28 | 8.015 | 7.04 | 1.12 | 1 | 3 | 3 | 0 | 0 | 20 |
| 0.6 | 0.3 | 0.1 | 0.23 | 127.4 | 701 | 13,964 | 28 | 8.015 | 7.04 | 1.12 | 1 | 3 | 3 | 0 | 0 | 20 |
| 0.6 | 0.2 | 0.2 | 0.27 | 120.3 | 1,382 | 175,127 | 31 | 5.075 | 5.1 | 3.11 | 0.5 | 5 | 2 | 0 | 0 | 19 |
| 0.6 | 0.1 | 0.3 | 0.18 | 134.0 | 1,417 | 263,272 | 31 | 3.14 | 3.15 | 1.11 | 0.4 | 0 | 0 | 0 | 0 | 20 |
| 0.6 | 0 | 0.4 | 0.08 | 134.0 | 1,417 | 263,272 | 31 | 3.14 | 3.15 | 1.11 | 0.4 | 0 | 0 | 0 | 0 | 20 |
| 0.5 | 0.5 | 0 | 0.19 | 127.4 | 701 | 13,964 | 28 | 8.015 | 7.04 | 1.12 | 1 | 3 | 3 | 0 | 0 | 20 |
| 0.5 | 0.4 | 0.1 | 0.25 | 127.4 | 701 | 13,964 | 28 | 8.015 | 7.04 | 1.12 | 1 | 3 | 3 | 0 | 0 | 20 |
| 0.5 | 0.3 | 0.2 | 0.32 | 127.4 | 701 | 13,964 | 28 | 8.015 | 7.04 | 1.12 | 1 | 3 | 3 | 0 | 0 | 20 |
| 0.5 | 0.2 | 0.3 | 0.27 | 134.0 | 1,417 | 263,272 | 31 | 3.14 | 3.15 | 1.11 | 0.4 | 0 | 0 | 0 | 0 | 20 |
| 0.5 | 0.1 | 0.4 | 0.17 | 134.0 | 1,417 | 263,272 | 31 | 3.14 | 3.15 | 1.11 | 0.4 | 0 | 0 | 0 | 0 | 20 |
| 0.5 | 0 | 0.5 | 0.08 | 134.0 | 1,417 | 263,272 | 31 | 3.14 | 3.15 | 1.11 | 0.4 | 0 | 0 | 0 | 0 | 20 |
| 0.4 | 0.6 | 0 | 0.22 | 127.4 | 701 | 13,964 | 28 | 8.015 | 7.04 | 1.12 | 1 | 3 | 3 | 0 | 0 | 20 |
| 0.4 | 0.5 | 0.1 | 0.28 | 127.4 | 701 | 13,964 | 28 | 8.015 | 7.04 | 1.12 | 1 | 3 | 3 | 0 | 0 | 20 |
| 0.4 | 0.4 | 0.2 | 0.34 | 127.4 | 701 | 13,964 | 28 | 8.015 | 7.04 | 1.12 | 1 | 3 | 3 | 0 | 0 | 20 |
| 0.4 | 0.3 | 0.3 | 0.35 | 134.0 | 1,417 | 263,272 | 31 | 3.14 | 3.15 | 1.11 | 0.4 | 0 | 0 | 0 | 0 | 20 |
| 0.4 | 0.2 | 0.4 | 0.26 | 134.0 | 1,417 | 263,272 | 31 | 3.14 | 3.15 | 1.11 | 0.4 | 0 | 0 | 0 | 0 | 20 |
| 0.4 | 0.1 | 0.5 | 0.16 | 134.0 | 1,417 | 263,272 | 31 | 3.14 | 3.15 | 1.11 | 0.4 | 0 | 0 | 0 | 0 | 20 |
| 0.4 | 0 | 0.6 | 0.07 | 134.0 | 1,417 | 263,272 | 31 | 3.14 | 3.15 | 1.11 | 0.4 | 0 | 0 | 0 | 0 | 20 |
| 0.3 | 0.7 | 0 | 0.23 | 209.1 | 409 | 7,548 | 10 | 3.08 | 3.11 | 6.05 | 0.3 | 5 | 0 | 0 | 0 | 18 |
| 0.3 | 0.6 | 0.1 | 0.31 | 127.4 | 701 | 13,964 | 28 | 8.015 | 7.04 | 1.12 | 1 | 3 | 3 | 0 | 0 | 20 |
| 0.3 | 0.5 | 0.2 | 0.37 | 127.4 | 701 | 13,964 | 28 | 8.015 | 7.04 | 1.12 | 1 | 3 | 3 | 0 | 0 | 20 |

| | | | | | | | | | | | | | | | | | |
|-----|-----|-----|------|-------|-------|---------|----|-------|------|-------|-----|---|---|---|---|---|----|
| 0.3 | 0.4 | 0.3 | 0.43 | 160.8 | 1,220 | 260,385 | 31 | 6.05 | 3.1 | 0 | 0.8 | 1 | 0 | 0 | 0 | 0 | 21 |
| 0.3 | 0.3 | 0.4 | 0.35 | 134.0 | 1,417 | 263,272 | 31 | 3.14 | 3.15 | 1.11 | 0.4 | 0 | 0 | 0 | 0 | 0 | 20 |
| 0.3 | 0.2 | 0.5 | 0.25 | 134.0 | 1,417 | 263,272 | 31 | 3.14 | 3.15 | 1.11 | 0.4 | 0 | 0 | 0 | 0 | 0 | 20 |
| 0.3 | 0.1 | 0.6 | 0.16 | 134.0 | 1,417 | 263,272 | 31 | 3.14 | 3.15 | 1.11 | 0.4 | 0 | 0 | 0 | 0 | 0 | 20 |
| 0.3 | 0 | 0.7 | 0.06 | 134.0 | 1,417 | 263,272 | 31 | 3.14 | 3.15 | 1.11 | 0.4 | 0 | 0 | 0 | 0 | 0 | 20 |
| 0.2 | 0.8 | 0 | 0.15 | 228.4 | 355 | 19,333 | 10 | 4.13 | 3.15 | 5.065 | 0.6 | 6 | 0 | 0 | 0 | 0 | 19 |
| 0.2 | 0.7 | 0.1 | 0.25 | 228.4 | 355 | 19,333 | 10 | 4.13 | 3.15 | 5.065 | 0.6 | 6 | 0 | 0 | 0 | 0 | 19 |
| 0.2 | 0.6 | 0.2 | 0.34 | 228.4 | 355 | 19,333 | 10 | 4.13 | 3.15 | 5.065 | 0.6 | 6 | 0 | 0 | 0 | 0 | 19 |
| 0.2 | 0.5 | 0.3 | 0.44 | 228.4 | 355 | 19,333 | 10 | 4.13 | 3.15 | 5.065 | 0.6 | 6 | 0 | 0 | 0 | 0 | 19 |
| 0.2 | 0.4 | 0.4 | 0.41 | 160.8 | 1,220 | 260,385 | 31 | 6.05 | 3.1 | 0 | 0.8 | 1 | 0 | 0 | 0 | 0 | 21 |
| 0.2 | 0.3 | 0.5 | 0.33 | 160.8 | 1,220 | 260,385 | 31 | 6.05 | 3.1 | 0 | 0.8 | 1 | 0 | 0 | 0 | 0 | 21 |
| 0.2 | 0.2 | 0.6 | 0.24 | 154.1 | 1,389 | 276,182 | 31 | 8.005 | 1.09 | 3.02 | 0.6 | 0 | 0 | 0 | 0 | 0 | 20 |
| 0.2 | 0.1 | 0.7 | 0.15 | 154.1 | 1,389 | 276,182 | 31 | 8.005 | 1.09 | 3.02 | 0.6 | 0 | 0 | 0 | 0 | 0 | 20 |
| 0.2 | 0 | 0.8 | 0.05 | 154.1 | 1,389 | 276,182 | 31 | 8.005 | 1.09 | 3.02 | 0.6 | 0 | 0 | 0 | 0 | 0 | 20 |
| 0.1 | 0.9 | 0 | 0.08 | 228.4 | 355 | 19,333 | 10 | 4.13 | 3.15 | 5.065 | 0.6 | 6 | 0 | 0 | 0 | 0 | 19 |
| 0.1 | 0.8 | 0.1 | 0.17 | 228.4 | 355 | 19,333 | 10 | 4.13 | 3.15 | 5.065 | 0.6 | 6 | 0 | 0 | 0 | 0 | 19 |
| 0.1 | 0.7 | 0.2 | 0.26 | 228.4 | 355 | 19,333 | 10 | 4.13 | 3.15 | 5.065 | 0.6 | 6 | 0 | 0 | 0 | 0 | 19 |
| 0.1 | 0.6 | 0.3 | 0.36 | 228.4 | 355 | 19,333 | 10 | 4.13 | 3.15 | 5.065 | 0.6 | 6 | 0 | 0 | 0 | 0 | 19 |
| 0.1 | 0.5 | 0.4 | 0.45 | 228.4 | 355 | 19,333 | 10 | 4.13 | 3.15 | 5.065 | 0.6 | 6 | 0 | 0 | 0 | 0 | 19 |
| 0.1 | 0.4 | 0.5 | 0.38 | 160.8 | 1,220 | 260,385 | 31 | 6.05 | 3.1 | 0 | 0.8 | 1 | 0 | 0 | 0 | 0 | 21 |
| 0.1 | 0.3 | 0.6 | 0.31 | 160.8 | 1,220 | 260,385 | 31 | 6.05 | 3.1 | 0 | 0.8 | 1 | 0 | 0 | 0 | 0 | 21 |
| 0.1 | 0.2 | 0.7 | 0.22 | 154.1 | 1,389 | 276,182 | 31 | 8.005 | 1.09 | 3.02 | 0.6 | 0 | 0 | 0 | 0 | 0 | 20 |
| 0.1 | 0.1 | 0.8 | 0.12 | 154.1 | 1,389 | 276,182 | 31 | 8.005 | 1.09 | 3.02 | 0.6 | 0 | 0 | 0 | 0 | 0 | 20 |
| 0.1 | 0 | 0.9 | 0.02 | 154.1 | 1,389 | 276,182 | 31 | 8.005 | 1.09 | 3.02 | 0.6 | 0 | 0 | 0 | 0 | 0 | 20 |
| 0 | 1 | 0 | 0.00 | 228.4 | 355 | 19,333 | 10 | 4.13 | 3.15 | 5.065 | 0.6 | 6 | 0 | 0 | 0 | 0 | 19 |
| 0 | 0.9 | 0.1 | 0.09 | 228.4 | 355 | 19,333 | 10 | 4.13 | 3.15 | 5.065 | 0.6 | 6 | 0 | 0 | 0 | 0 | 19 |
| 0 | 0.8 | 0.2 | 0.19 | 228.4 | 355 | 19,333 | 10 | 4.13 | 3.15 | 5.065 | 0.6 | 6 | 0 | 0 | 0 | 0 | 19 |
| 0 | 0.7 | 0.3 | 0.28 | 228.4 | 355 | 19,333 | 10 | 4.13 | 3.15 | 5.065 | 0.6 | 6 | 0 | 0 | 0 | 0 | 19 |
| 0 | 0.6 | 0.4 | 0.37 | 228.4 | 355 | 19,333 | 10 | 4.13 | 3.15 | 5.065 | 0.6 | 6 | 0 | 0 | 0 | 0 | 19 |
| 0 | 0.5 | 0.5 | 0.44 | 160.8 | 1,220 | 260,385 | 31 | 6.05 | 3.1 | 0 | 0.8 | 1 | 0 | 0 | 0 | 0 | 21 |
| 0 | 0.4 | 0.6 | 0.36 | 160.8 | 1,220 | 260,385 | 31 | 6.05 | 3.1 | 0 | 0.8 | 1 | 0 | 0 | 0 | 0 | 21 |
| 0 | 0.3 | 0.7 | 0.28 | 160.8 | 1,220 | 260,385 | 31 | 6.05 | 3.1 | 0 | 0.8 | 1 | 0 | 0 | 0 | 0 | 21 |
| 0 | 0.2 | 0.8 | 0.19 | 154.1 | 1,389 | 276,182 | 31 | 8.005 | 1.09 | 3.02 | 0.6 | 0 | 0 | 0 | 0 | 0 | 20 |
| 0 | 0.1 | 0.9 | 0.10 | 154.1 | 1,389 | 276,182 | 31 | 8.005 | 1.09 | 3.02 | 0.6 | 0 | 0 | 0 | 0 | 0 | 20 |
| 0 | 0 | 1 | 0.00 | 154.1 | 1,389 | 276,182 | 31 | 8.005 | 1.09 | 3.02 | 0.6 | 0 | 0 | 0 | 0 | 0 | 20 |

966 **References**

- 967 [1] Dincer I, Zamfirescu C. Sustainable Energy Systems and Applications. US: Springer 2012.
- 968 [2] Miller C, Hersberger C, Jones M. Automation of common building energy simulation
969 workflows using python In: IBPSA editor. Conference Automation of common building energy
970 simulation workflows using python, Chambéry, France. p. 210-7.
- 971 [3] LBNL, USDOE. DOE-2. James J. Hirsch & Associates 2015.
- 972 [4] EnergyPlus. EnergyPlus Engineering Reference. 2012. p. 1278.
- 973 [5] Chuah JW, Raghunathan A, Jha NK. ROBESim: A retrofit-oriented building energy
974 simulator based on EnergyPlus. Energy and Buildings. 2013;66(0):88-103.
- 975 [6] Hong T, Piette MA, Chen Y, Lee SH, Taylor-Lange SC, Zhang R, et al. Commercial Building
976 Energy Saver: An energy retrofit analysis toolkit. Applied Energy. 2015;159:298-309.
- 977 [7] Mauro GM, Hamdy M, Vanoli GP, Bianco N, Hensen JLM. A new methodology for
978 investigating the cost-optimality of energy retrofitting a building category. Energy and
979 Buildings. 2015;107:456-78.
- 980 [8] Rysanek AM, Choudhary R. Optimum building energy retrofits under technical and
981 economic uncertainty. Energy and Buildings. 2013;57(0):324-37.
- 982 [9] Klein SA. TRNSYS 17: A Transient System Simulation Program. In: Solar Energy
983 Laboratory UoW, editor. Madison, USA2010.
- 984 [10] The MathWorks. MATLAB and Statistics Toolbox Release 2012b. Natick, Massachusetts,
985 United States.2012.
- 986 [11] Nguyen A-T, Reiter S, Rigo P. A review on simulation-based optimization methods applied
987 to building performance analysis. Applied Energy. 2014;113(0):1043-58.
- 988 [12] Attia S, Hamdy M, O'Brien W, Carlucci S. Assessing gaps and needs for integrating
989 building performance optimization tools in net zero energy buildings design. Energy and
990 Buildings. 2013;60(0):110-24.
- 991 [13] Siddharth V, Ramakrishna PV, Geetha T, Sivasubramaniam A. Automatic generation of
992 energy conservation measures in buildings using genetic algorithms. Energy and Buildings.
993 2011;43(10):2718-26.
- 994 [14] Asadi E, da Silva MG, Antunes CH, Dias L. Multi-objective optimization for building retrofit
995 strategies: A model and an application. Energy and Buildings. 2012;44(0):81-7.
- 996 [15] Malatji EM, Zhang J, Xia X. A multiple objective optimisation model for building energy
997 efficiency investment decision. Energy and Buildings. 2013;61(0):81-7.
- 998 [16] Diakaki C, Grigoroudis E, Kolokotsa D. Towards a multi-objective optimization approach
999 for improving energy efficiency in buildings. Energy and Buildings. 2008;40(9):1747-54.
- 1000 [17] Tsatsaronis G. Exergoeconomics and Exergoenvironmental Analysis. In: Bakshi BR,
1001 Gutowski TG, Sekulic DP, editors. Thermodynamics and the Destruction of Resources:
1002 Cambridge University Press; 2014.
- 1003 [18] Hammond GP, Stapleton AJ. Exergy analysis of the United Kingdom energy system.
1004 Proceedings of the Institution of Mechanical Engineers, Part A: Journal of Power and Energy.
1005 2001;215(2):141-62.
- 1006 [19] Gasparatos A, El-Haram M, Horner M. Assessing the sustainability of the UK society using
1007 thermodynamic concepts: Part 2. Renewable and Sustainable Energy Reviews.
1008 2009;13(5):956-70.

- 1009 [20] Streich M. Opportunities and limits for exergy analysis in cryogenics. *Chemical*
1010 *Engineering & Technology*. 1996;19:498-502.
- 1011 [21] Lior N. Thoughts about future power generation systems and the role of exergy analysis
1012 in their development. *Energy Conversion and Management*. 2002;43:1187-98.
- 1013 [22] Montelongo-Luna JM, Svrcek WY, Young BR. An exergy calculator tool for process
1014 simulation. *Asia-Pacific Journal of Chemical Engineering*. 2007;2:431-7.
- 1015 [23] Querol E, Gonzalez-Regueral B, Ramos A, Perez-Benedito JL. Novel application for
1016 exergy and thermoeconomic analysis of processes simulated with Aspen Plus®. *Energy*.
1017 2011;36:964-74.
- 1018 [24] Suleman F, Dincer I, Agelin-Chaab M. Energy and exergy analyses of an integrated solar
1019 heat pump system. *Applied Thermal Engineering*. 2014;73:559-66.
- 1020 [25] Ghannadzadeh A, Thery-Hetreux R, Baudouin O, Baudet P, Floquet P, Joulia X. General
1021 methodology for exergy balance in ProSimPlus® process simulator. *Energy*. 2012;44:38-59.
- 1022 [26] Fisk D. Optimising heating system structure using exergy Branch and Bound. *Building*
1023 *Services Engineering Research and Technology*. 2014;35(3):321-33.
- 1024 [27] EBC-Annex37. Technical Synthesis Report: Low Exergy Systems for Heating and Cooling
1025 of Buildings, IEA ECBCS. In: Jagpal R, editor. UK2007.
- 1026 [28] Sakulpipatsin P, Schmidt D. Exergy analysis applied to building design. 2005:8.
- 1027 [29] EBC-Annex49. Detailed Exergy Assessment Guidebook for the Built Environment, IEA
1028 ECBCS. In: Torio H, Schmidt D, editors.: Fraunhofer IBP; 2011.
- 1029 [30] Schlueter A, Thesseling F. Building information model based energy/exergy performance
1030 assessment in early design stages. *Automation in Construction*. 2009;18(2):153-63.
- 1031 [31] Sakulpipatsin P, Itard LCM, van der Kooi HJ, Boelman EC, Luscuere PG. An exergy
1032 application for analysis of buildings and HVAC systems. *Energy and Buildings*. 2010;42(1):90-
1033 9.
- 1034 [32] Angelotti A, Caputo P, Solani G. Dynamic exergy analysis of an air source heat pump. 1st
1035 International Exergy, Life Cycle Assessment, and Sustainability Workshop & Symposium
1036 (ELCAS). 2009:8.
- 1037 [33] Tsatsaronis G, Park M-H. On avoidable and unavoidable exergy destructions and
1038 investment costs in thermal systems. *Energy Conversion and Management*. 2002;43:1259-70.
- 1039 [34] Rocco MV, Colombo E, Sciubba E. Advances in exergy analysis: a novel assessment of
1040 the Extended Exergy Accounting method. *Applied Energy*. 2014;113:1405-20.
- 1041 [35] Wall G. Exergy - a useful concept within resource accounting. 1977(Report no. 77-42,
1042 Institute of Theoretical Physics, Chalmers University of Technology and University of
1043 Göteborg).
- 1044 [36] Kohl T, Teles M, Melin K, Laukkanen T, Järvinen M, Park SW, et al. Exergoeconomic
1045 assessment of CHP-integrated biomass upgrading. *Applied Energy*. 2015;156:290-305.
- 1046 [37] Mosaffa AH, Garousi Farshi L. Exergoeconomic and environmental analyses of an air
1047 conditioning system using thermal energy storage. *Applied Energy*. 2016;162:515-26.
- 1048 [38] Wang X, Dai Y. Exergoeconomic analysis of utilizing the transcritical CO₂ cycle and the
1049 ORC for a recompression supercritical CO₂ cycle waste heat recovery: A comparative study.
1050 *Applied Energy*. 2016;170:193-207.
- 1051 [39] Valero A, Torres C. Thermoeconomic Analysis. In: Frangopoulos CA, editor. *Exergy,*
1052 *energy system analysis, and optimization: EOLSS*; 2009. p. 454.

- 1053 [40] Valdés M, Durán MD, Rovira A. Thermo-economic optimization of combined cycle gas
1054 turbine power plants using genetic algorithms. *Applied Thermal Engineering*. 2003;23:2169-
1055 82.
- 1056 [41] Mofid G-B, Hamed G. Exergoeconomic optimization of gas turbine power plants operating
1057 parameters using genetic algorithms: A case study. *Thermal Science* 2011;15:43-54.
- 1058 [42] Ahmadi P, Dincer I, Rosen MA. Thermodynamic modeling and multi-objective
1059 evolutionary-based optimization of a new multigeneration energy system. *Energy Conversion*
1060 *and Management*. 2013;76:282-300.
- 1061 [43] Dong R, Yu Y, Zhang Z. Simultaneous optimization of integrated heat, mass and pressure
1062 exchange network using exergoeconomic method. *Applied Energy*. 2014;136:1098-109.
- 1063 [44] Sadeghi M, Chitsaz A, Mahmoudi SMS, Rosen MA. Thermo-economic optimization using
1064 an evolutionary algorithm of a trigeneration system driven by a solid oxide fuel cell. *Energy*.
1065 2015;89:191-204.
- 1066 [45] Baghsheikhi M, Sayyaadi H. Real-time exergoeconomic optimization of a steam power
1067 plant using a soft computing-fuzzy inference system. *Energy*. 2016;114:868-84.
- 1068 [46] Deslauriers M-A, Sorin M, Marcos B, Richard M-A. Retrofit of low-temperature heat
1069 recovery industrial systems using multiobjective exergoeconomic optimization. *Energy*
1070 *Conversion and Management*. 2016;130:207-18.
- 1071 [47] Xia J, Wang J, Lou J, Zhao P, Dai Y. Thermo-economic analysis and optimization of a
1072 combined cooling and power (CCP) system for engine waste heat recovery. *Energy*
1073 *Conversion and Management*. 2016;128:303-16.
- 1074 [48] Ozcan H, Dincer I. Exergoeconomic optimization of a new four-step magnesium–chlorine
1075 cycle. *International Journal of Hydrogen Energy*. 2017.
- 1076 [49] Tozer R, Lozano Serrano MA, Valero Capilla A, James R. Thermo-economics applied to
1077 an air conditioning system with cogeneration. *Building Services Engineering Research and*
1078 *Technology*. 1996;17(1):37-42.
- 1079 [50] Tozer R, James R. Thermo-economic life-cycle costs of absorption chillers. *Building*
1080 *Services Engineering Research and Technology*. 1997;18(3):149-55.
- 1081 [51] Ozgener O, Hepbasli A, Dincer I, Rosen MA. Modelling and assessment of ground-source
1082 heat pump systems using exergoeconomic analysis for building applications. Ninth
1083 International IBPSA Conference Montréal, Canada. 2005:15–8.
- 1084 [52] Ucar A. Thermo-economic analysis method for optimization of insulation thickness for the
1085 four different climatic regions of Turkey. *Energy*. 2010;35(4):1854-64.
- 1086 [53] Caliskan H, Dincer I, Hepbasli A. Thermo-economic analysis of a building energy system
1087 integrated with energy storage options. *Energy Conversion and Management*. 2013;76(0):274-
1088 81.
- 1089 [54] Baldvinsson I, Nakata T. A comparative exergy and exergoeconomic analysis of a
1090 residential heat supply system paradigm of Japan and local source based district heating
1091 system using SPECO (specific exergy cost) method. *Energy*. 2014;74:537-54.
- 1092 [55] Yücer CT, Hepbasli A. Exergoeconomic and enviroeconomic analyses of a building
1093 heating system using SPECO and Lowex methods. *Energy and Buildings*. 2014;73(0):1-6.
- 1094 [56] Akbulut U, Utlu Z, Kincay O. Exergoenvironmental and exergoeconomic analyses of a
1095 vertical type ground source heat pump integrated wall cooling system. *Applied Thermal*
1096 *Engineering*. 2016;102:904-21.
- 1097 [57] García Kerdan I, Raslan R, Ruyssevelt P. An exergy-based multi-objective optimisation
1098 model for energy retrofit strategies in non-domestic buildings. *Energy*. 2016;117, Part 2:506-
1099 22.

- 1100 [58] García Kerdan I, Raslan R, Ruyssevelt P, Morillón Gálvez D. An exergoeconomic-based
1101 parametric study to examine the effects of active and passive energy retrofit strategies for
1102 buildings. *Energy and Buildings*. 2016;133:155-71.
- 1103 [59] Torio H. Comparison and optimization of building energy supply systems through exergy
1104 analysis and its perspectives: Fraunhofer, 2012.
- 1105 [60] Rosen M, Bulucea CA. Using Exergy to Understand and Improve the Efficiency of
1106 Electrical Power Technologies. *Entropy*. 2009;11(4):820-35.
- 1107 [61] Lazzaretto A, Tsatsaronis G. SPECO: A systematic and general methodology for
1108 calculating efficiencies and costs in thermal systems. *Energy*. 2006;31(8–9):1257-89.
- 1109 [62] Tsatsaronis G. Thermo-economic analysis and optimization of energy systems. *Progress
1110 in Energy and Combustion Science*. 1993;19(3):227-57.
- 1111 [63] Ma Z, Cooper P, Daly D, Ledo L. Existing building retrofits: Methodology and state-of-the-
1112 art. *Energy and Buildings*. 2012;55(0):889-902.
- 1113 [64] SimLab 2.2. Simulation environment for uncertainty and sensitivity analysis. . Joint
1114 Research Center of the European Commission.; 2011.
- 1115 [65] Python Software Foundation. Python Language Reference version 2.7.
- 1116 [66] JEPlus 1.6. JEPlus – An EnergyPlus simulation manager for parametrics. 2016.
- 1117 [67] JEPlus+EA 1.7. Building Design Optimization using JEPlus. 2016.
- 1118 [68] CIBSE. Guide A: Environmental Design. In: Engineers CloBS, editor. London, UK2015.
- 1119 [69] ASHRAE. ANSI/ASHRAE Standard 55-2004. Thermal Environmental Conditions for
1120 Human Occupancy. American Society of Heating, Refrigerating and Air-conditioning
1121 Engineers; 2004.
- 1122 [70] Korolija I, Marjanovic-Halburd L, Zhang Y, Hanby VI. UK office buildings archetypal model
1123 as methodological approach in development of regression models for predicting building
1124 energy consumption from heating and cooling demands. *Energy and Buildings*.
1125 2013;60(0):152-62.
- 1126 [71] CIBSE. Guide F: Energy Efficiency in Buildings. In: Engineers CloBS, editor. London,
1127 UK2012.
- 1128 [72] ARUP. Low Carbon Routemap for the UK Built Environment. In: Board TGC, editor.
1129 UK2013.
- 1130 [73] Haupt RL, Haupt SE. *Practical Genetic Algorithms*. 2nd ed: Wiley, 2004.
- 1131 [74] BRE. National Calculation Methodology (NCM) modelling guide (for buildings other than
1132 dwellings in England and Wales). 2010 Edition. In: (BRE, editor. Department for Communities
1133 and Local Government2013. p. 34.
- 1134 [75] Bull J, Gupta A, Mumovic D, Kimpian J. Life cycle cost and carbon footprint of energy
1135 efficient refurbishments to 20th century UK school buildings. *International Journal of
1136 Sustainable Built Environment*. 2015.